Offshore ADCP deployments (Otago Peninsula) for Port of Otago dredging project

NIWA Client Report: HAM2008-178
November 2008

NIWA Project: POL08202

Offshore ADCP deployments (Otago Peninsula) for Port Otago dredging project

R.G. Bell
C. Hart

NIWA contact/Corresponding author

R.G. Bell

Prepared for

Port Otago Ltd

NIWA Client Report: HAM2008-178
November 2008

NIWA Project: POL08202

National Institute of Water & Atmospheric Research Ltd
Gate 10, Silverdale Road, Hamilton
P O Box 11115, Hamilton, New Zealand
Phone +64-7-856 7026, Fax +64-7-856 0151
www.niwa.co.nz

Contents

Reviewed by:

R.M. Gorman

Approved for release by:

M.O. Green

Formatting checked

A. Bartley

Executive Summary

As part of Next Generation, Port Otago Ltd (POL) commissioned NIWA to carry out a field programme deploying current and wave instruments to support hydrodynamic and wave model studies in shelf waters off Otago Harbour. Both the field investigations and the subsequent model studies (reported separately) were undertaken to underpin an assessment of the effects of channel deepening and dredging operations on Otago Harbour and the effects of dredged material disposal on the inner shelf environment.

A full set of current and wave measurements has been obtained at a potential dredged-material disposal site at A1 (4 km northeast of Taiaroa Head) over a 4 month period from March to July 2008 (excluding gaps between deployments). For all but one of these deployments, a concurrent ADCP mooring site was also occupied at either B1 (Blueskin Bay) or B2 (Heyward Point). Inshore, waves were only measured at B2, due to a malfunction in the ADCP at site B1. The range of winds experienced during the field programme was not too dissimilar to the long-term average distribution from the long-term record at Taiaroa Head, but there were slightly more west to south-west winds, offset mainly by slightly less winds from the north-east quadrant. Strong winds from the south-east are infrequent, but one event was measured in the last deployment, which provides insight into current flows that coincide with large waves, with the potential for high sediment transport rates.

This Report presents a detailed synthesis of the field measurements and draws out the key oceanographic and meteorological factors that explain the variability and extremes in the ADCP datasets.

The current velocity measurements provide a useful dataset in their own right showing the prevailing patterns of coastal and shelf circulation in the area of Otago Heads. Tidal currents at all three ADCP sites only accounted for a small proportion of the measured currents—instead winds combined with the influence of the Southland Current are the main drivers for currents. At A1, the prevailing current drift in most cases is to the SE, with a slight deviation to the south in the last deployment (July 2008). This prevailing current drift is altered at times when moderate to strong S to SE winds reverse the net drift, but otherwise the more frequent winds from the SW and NE quadrants appear to sustain the south-easterly drift. Sometimes winds from a more northerly direction cause this current drift to deviate slightly more towards the south at A1.

These results have implications for the hydrodynamic and sediment modelling for a disposal ground offshore (Bell et al. 2009), with tides being negligible, the Southland Current providing the regional driver of net (average) flow patterns (including the possibility of an eddy off Otago Heads), and the winds being the predominant cause of variability of current drift in the area of the offshore site A1.

In Blueskin Bay (B1), the net current drift was quite variable. For the first deployment in March/April 2008, the current drift exhibited slow cyclic meanders at the seabed arising from a succession of alternate NE and SW winds. This contrasts with the June 2008 deployment, where the current drift was more consistently towards the northerly quarter, due to more frequent and stronger winds from the SW and weaker less frequent winds from the NE.

Off Heyward Point (B2), the prevailing net current drift is generally eastwards at 1 km/day near the seabed. In a similar manner to site A1, S to SE winds can reverse the net drift at B2 to be in a more NW direction towards Blueskin Bay.

The current velocity measurements at various depths provide a reliable and consistent dataset for use in hydrodynamic, sediment-plume and sediment-transport models used to assess environmental effects in Bell et al. (2009).

Logged temperatures and some salinity-depth profiling indicated that weak density stratification can be present at times e.g., heating of surface waters in autumn and a small signature of reduced surface salinities (probably from the Clutha River). However, it was mainly confined to the top few metres of the water column, and is unlikely to affect the dispersal of dredged material released at the disposal site from a dredger with a draught of several metres. Temperature measurements were also used to bracket winter and late-summer estimates of settling velocity for sediment grains, with settling slightly slower in colder temperatures.

The three highest wave events for the field season all occurred during the last deployment. The highest significant wave height of 4.7 m was reached at 1800 h on 31 July 2008, with peak spectral periods of 11–13 seconds (swell) arriving from an easterly direction. Local winds at Taiaroa Head preceding this wave peak were from the SE. The second highest significant wave height of 4.5 m was reached a week earlier at 0600 h on 24 July 2008, with peak spectral periods of 10–12 seconds (swell) arriving from a SE direction, with local winds blowing from the S.

Wave statistics measured at A1 provide an essential dataset to verify wave models, which subsequently are required as input to sediment-transport models. The wave information also provides a future resource for verifying any future wave forecasting system for the port operations.

Overall, these field datasets provide a coherent picture of the prevailing currents, waves and their variability in response to wind forcing on the inner shelf off Otago Heads. The extension of the field programme to a fourth deployment was worthwhile, capturing the three largest wave events for the entire field programme and providing useful insights on the current drift offshore at site A1 when infrequent winds blow from the SE.

1. Introduction

1.1 Background

Project Next Generation is an initiative by Port Otago Ltd. (POL) to expand the capability of Port Chalmers through a substantial channel deepening capital works programme.

As part of Next Generation, POL commissioned NIWA to carry out a field programme deploying current and wave instruments to support hydrodynamic and wave model studies in shelf waters off Otago Harbour. Both field and model studies were undertaken to underpin an assessment of the effects of channel deepening and dredging/disposal operations on the harbour and offshore environments.

The offshore field programme was complemented by the deployment of a current meter at three successive locations within the harbour by the Dept. of Marine Science, University of Otago (Bowman, 2008a,b) and by tide and wind measurements from POL operational tide and wind gauges located at The Spit Wharf, Port Chalmers and Dunedin Wharf.

1.2 Report content and purpose

This report provides a summary of the tide, current, wave and temperature measurements recorded during the offshore field programme covering the period from 18 March to 4 August 2008 (nominally 20 weeks). The contract was for an initial 3 month period, but was extended to capture a longer season of wave and net-current drift data that covered both autumn and the winter storm period.

The Report provides POL and various stakeholders with an overall summary of the field data collected offshore around Otago Heads and a brief synthesis of the main results. The other primary purpose of the data was to support the development of numerical models of current flow, sediment transport and suspended-sediment plume dispersion, which are described in Bell et al. (2009). The offshore wave data were provided to MetOcean Ltd, who were contracted separately by POL to provide wave modelling services to the project.

2. Deployment information

2.1 ADCPs

The primary instrument used was an RDI Acoustic Doppler Current Profiler (ADCP), which measure currents in various depth bins above the bottom-mounted acoustic sensors. Each ADCP was also equipped with a wave module to enable the ADCP to measure wave parameters via a pressure sensor, surface reflection characteristics and the wave orbital currents. An RDI ADCP is shown in Figure 2.1.

Figure 2.1: Looking down on the acoustic sensor head of an internal-recording RDI Acoustic Doppler Current Profiler (ADCP).

The ADCPs were deployed in weighted mooring frames that were lowered to the seabed and tethered to a surface buoy and navigation light as shown in the schematic mooring configuration in Figure 2.2. The acoustic head was nominally 0.4 m above the seabed. Resource consents for the moorings were obtained from Otago Regional Council.

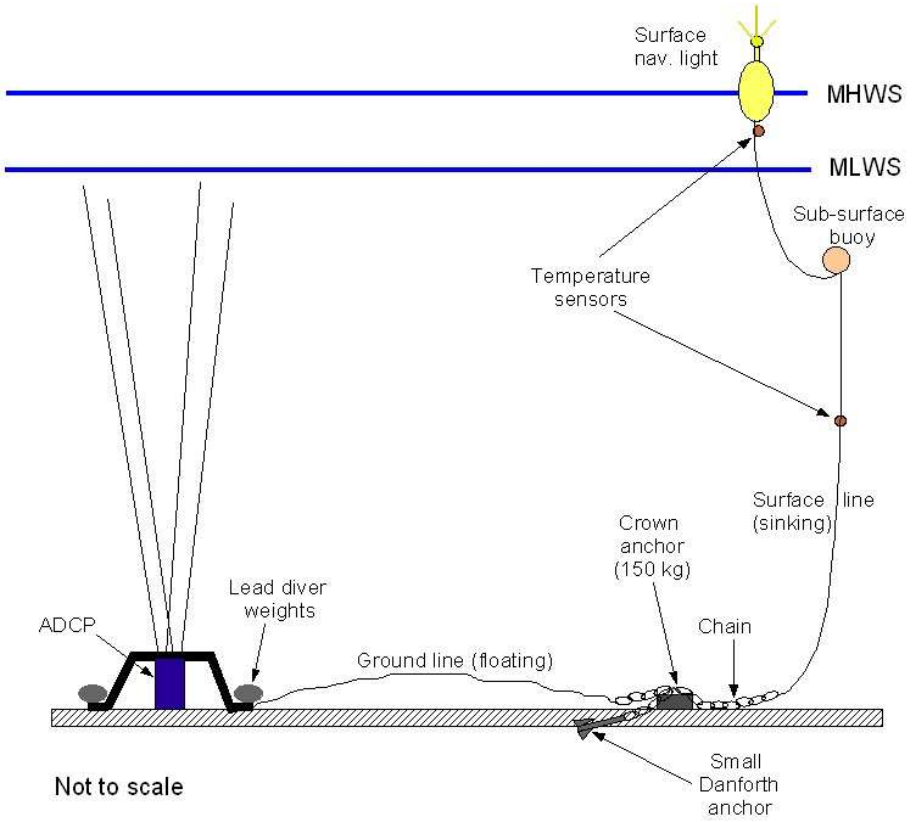

Figure 2.2: Schematic diagram of an ADCP mooring configuration used off Otago Peninsula.

One of the ADCPs was moored in the centre of one of the proposed disposal sites in 30 m depth of water 4 km northeast of Taiaroa Head (A1) and the other ADCP was moored inshore occupying two different sites—initially off Warrington in Blueskin Bay (B1) and later at the start of July off Heyward Point (B2). Locations and deployment periods are provided in Table 2.1. The sites are mapped in Figure 2.3.

Table 2.1: Locations (WGS-84) and times for the ADCP deployments.

Site/Deployment #	Latitude (S)	Longitude (E)	Time period in NZST (in water)
B1 /1	45°42.463	170°38.286	1840 18 Mar to 0750 0 4 Apr 2008
B1 /2	"	"	No deployment (due to malfunction)
B1 /3	"	"	1600 31 May to 1040 29 Jun 2008
B2 /1	45°45.129	170°42.343	1020 04 July to 1350 04 Aug 2008
A1 /1	45°44.695	170°45.716	1710 18 Mar to 1230 21 Apr 2008
A1 /2	"	"	0720 29-Apr to 1600 26 May 2008
A1 /3	"	"	1620 31-May to 1400 29-Jun 2008
A1 /4	"	"	0950 04 July to 1500 04 Aug 2008

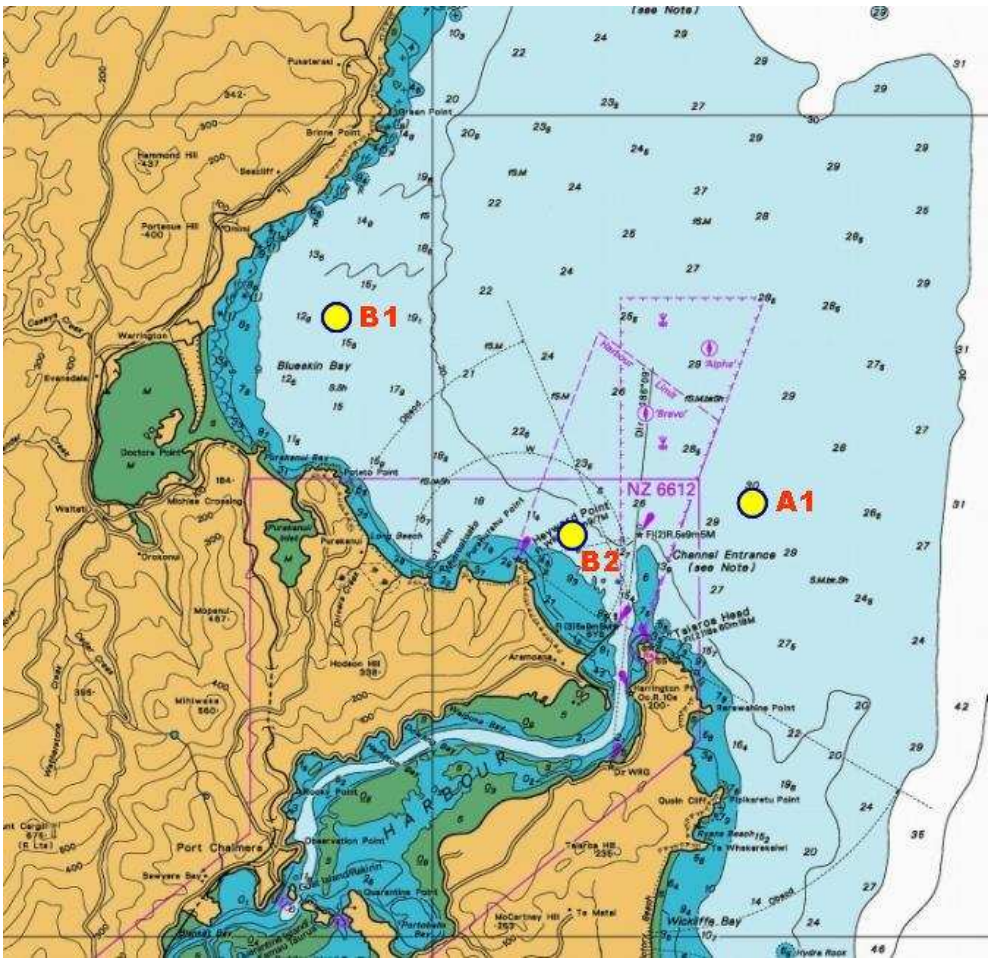

Figure 2.3: Location map of the three ADCP mooring sites occupied during the offshore field programme. [*Source of map: extracted from Chart NZ661, Approaches to Otago Harbour, ©Land Information NZ, 2006*].

The main parameters for each deployment are listed in Table 2.2. Currents in each vertical bin were averaged over 10 minute periods from 48 acoustic pings at 12.5 second intervals.

Waves were extracted from 20-minute bursts at a 2 Hz sampling rate every 2 hours, except for deployment A1 /1 when the bursts were measured every hour (but subsequently increased to 2 hour intervals thereafter to conserve battery power). Wave statistics were derived primarily from the wave-orbital velocities measured in the upper water column. Back-up measurements of wave height via the pressure (depth) sensor were generally not appropriate to use in this situation because of the depth of water above the depth sensor other than during high, long-period swells.

Table 2.2: ADCP deployment parameters.

Site/Deployment #	Instrument No. & freq	Mean water depth to sensors (m)	Vertical bin size (m)	Waves
B1 /1	#5481 1200kHz	15.2	1.0	n/a
B1 /3	#1084 600kHz	15.25	0.75	✓
B2 /1	#1084 600kHz	15.3	0.75	✓
A1 /1	#7900 600kHz	30.9	0.75	✓
A1 /2	#7900 600kHz	31.0	0.75	✓
A1 /3	#7900 600kHz	31.0	0.75	✓
A1 /4	#7900 600kHz	30.5	0.75	✓

2.2 Sea temperature

Sea temperatures were measured to characterise typical temperatures in the shelf waters for input for estimating the range of settling velocities for sediment in the disposed sediment plumes. Sea-temperature depth profiles were also obtained as back-up information on the stratification in the water column in case the velocity measurements from the ADCPs exhibited vertical differences due to water-column stratification (which they didn't as it transpired).

Sea temperatures were measured by three different instruments: a) the ADCPs have a calibrated temperature sensor located on the main acoustic sensor head (which measured near-bed sea temperatures); b) HOBO Water Temperature Pro loggers on the two mooring lines near the surface buoy and at mid-water column; c) a Seabird

SBE 19 conductivity-temperature-depth (CTD) profiler which was used on 27 May 2008 between 1000 to 1040 hrs.

Of the 4 HOBO water temperature gauges deployed only two datasets were retrieved—the ones at the top and mid-depth of the B1/B2 mooring, with the mid-depth sensor at site A1 failing soon after deployment and the near-surface HOBO going missing (either through storm action or theft).

NIWA sea-surface temperature (SST) maps derived from NOAA satellites were also archived for the Otago shelf waters. These encompass the three locations for the ADCP deployments. An example SST map is shown in Figure 2.4. This illustrates the northward-flowing Southland Current which is comprised of two water bodies with an internal boundary between them called the Southland Front. To the east of the Front is the main body of the flow carrying cold Sub-Antarctic Water (blue-violet colours). Inshore of the Front is a lower-volume flow on the continental shelf of warmer water (red colours) arising from a portion of an eastward flow of Subtropical Water across the Tasman Sea that is deflected south around the New Zealand landmass and up the Otago shelf (Sutton, 2003). This latter portion of the Southland Current is warmer than waters found immediately adjacent to the coast during winter months (Figure 2.4).

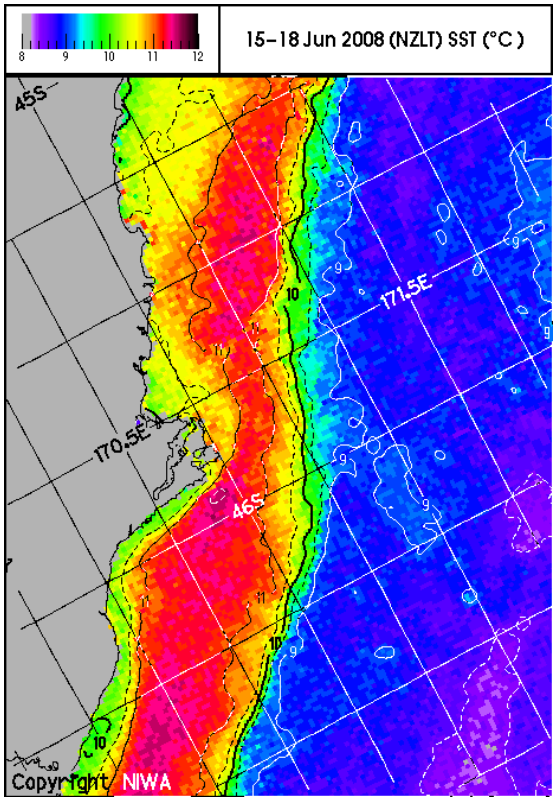

Figure 2.4: An example of NIWA's sea surface temperature (SST) maps integrated over a few days from NOAA satellite data—in this case integrated over the 15–18 June 2008. The

band of warmer waters in the mid-continental shelf region (red colours) is indicative of Subtropical Water carried north in the inshore section of the Southland Current.

2.3 Winds

Winds during the deployment period were obtained from the Automatic Weather Station at Taiaroa Head (NIWA Climate Database Agent No. 24854). The station is located 75 m above sea level.

2.4 Tides

Tide heights were measured by a pressure transducer on each ADCP relative to the acoustic sensor head. These were supplemented by tide gauge measurements from the Port Otago network (e.g., the Spit Jetty gauge at the entrance to Otago Harbour) and offshore sea level measurements at 1-minute intervals from NIWA's gauge on Green Island (45.956°S; 170.383°E) off Waldronville.

3. Wind and tide conditions

3.1 Winds

The long-term wind climate for Otago Heads area was derived from 10-minute averaged measurements at Taiaroa Head over the period January 1998 to May 2008, with a gap from November 2002 to May 2003. This spans approximately 10 years. The wind rose for wind speeds and directions for the 10-year period is shown in Figure 3.1.

The mean wind speed over the 10-year period was 7.1 m/s, with a maximum of 38 m/s reached on 3 May 2002 from the west. The wind directions exhibit a strong bi-modal distribution (Figure 3.1), dominated by winds from either the west to south-west or from the north to north-east.

The wind rose for the 2008 field deployment period is shown in Figure 3.2 for the period 19 March to 4 August. The mean wind speed over the field period was 6.7 m/s (slightly lower than the 10-year average) with slightly higher occurrence of calm conditions (4.2% versus 2%). The maximum was 29.3 m/s, which was recorded on 18 April 2008 from the west (260°). The overall distribution and pattern of wind directions during the field deployment is similar to the long-term climate (comparing Figure 3.1 with 3.2). However, there were slightly more west to south-west winds[1] (45% during the field period compared with 41% in long-term climate) offset mainly by slightly less winds from the north-east quadrant[2] (39% occurrence in field period versus 42% in long-term climate). This means the range of winds experienced during the field programme was not too dissimilar to the long-term average distribution.

Individual wind time series (wind speed and direction) from Taiaroa Head for each ADCP deployment period are shown in Section 4 along with the current velocities to aid interpretation of the measurements.

[1] includes the 4 compass rose bars from SSW to W inclusive
[2] includes the 4 compass rose bars from N to ENE inclusive

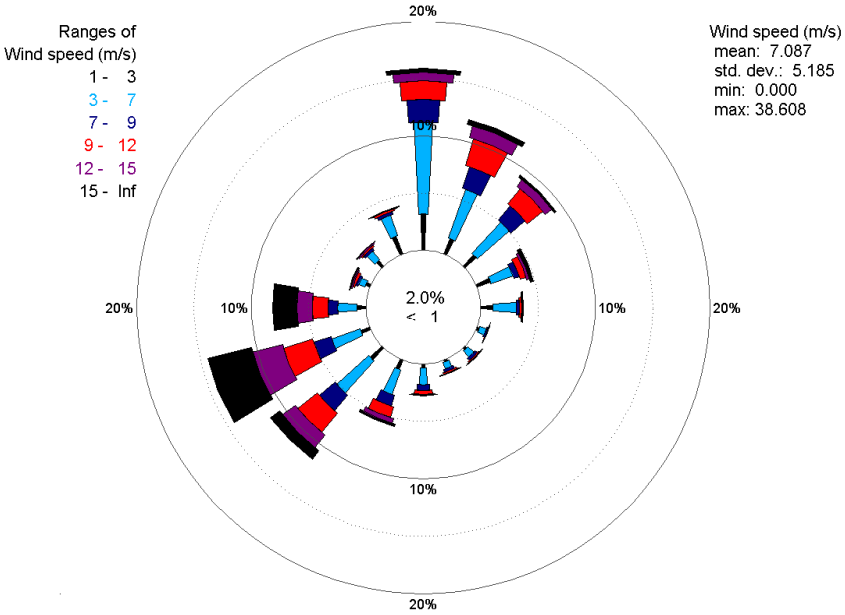

Figure 3.1: Wind rose for Taiaroa Head over the 10-year period from Jan 1998 to May 2008 (excl. 16 Nov 2002 to 17 May 2003). Wind speeds for each direction are accumulated by % occurrence in increasing increments of speed (indicated by the width of the bars). Meteorological convention is used in expressing the direction the wind "blows from".

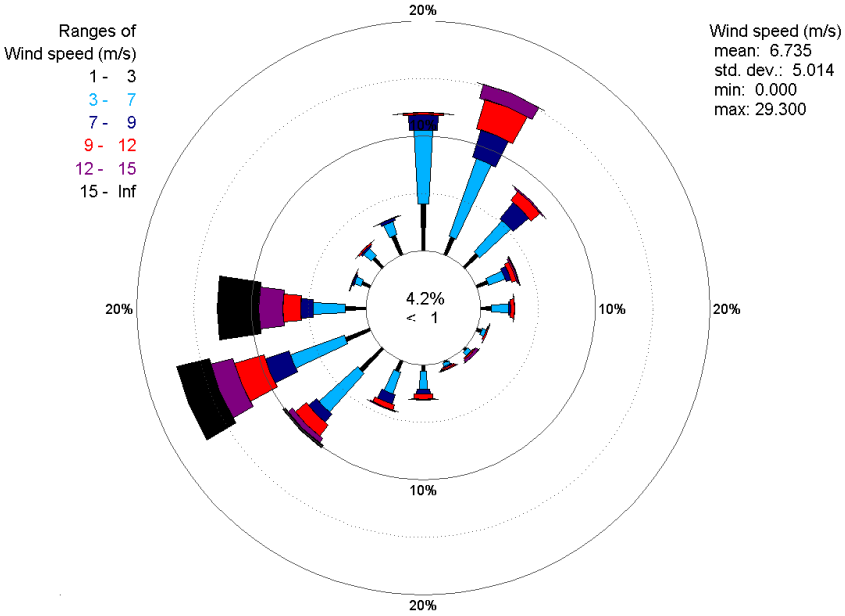

Figure 3.2: Wind rose that summarises the wind climate at Taiaroa Head for the 2008 field deployment period from 19 March to 04 August.

3.2 Tides

The tidal regime in Otago shelf waters is semi-diurnal (i.e., nominally two tides per day) with tide cycles of approximately 12.4 hours. The fortnightly spring/neap cycle is compounded by the monthly perigean-apogean tide cycle, which arises from the Moon's elliptical, rather than circular, orbit around the Earth.

The sea-level time series from NIWA's gauge (site 74099) on Green Island (south of Waldronville) for the field deployment are shown in Figure 3.3 in a series of 4 plots, one for each ADCP deployment period. The highest water level was reached on 7 June, during a storm-tide event associated with a barometric pressure drop to 996 hPa and SW winds of up to 20 m/s.

Tides recorded at the Spit Wharf Jetty from March to July 2008 were used to drive the Harbour model from an open-sea boundary to verify the model calibration based on previous field programmes in 1988 and 1998 (Bell et al. 2009).

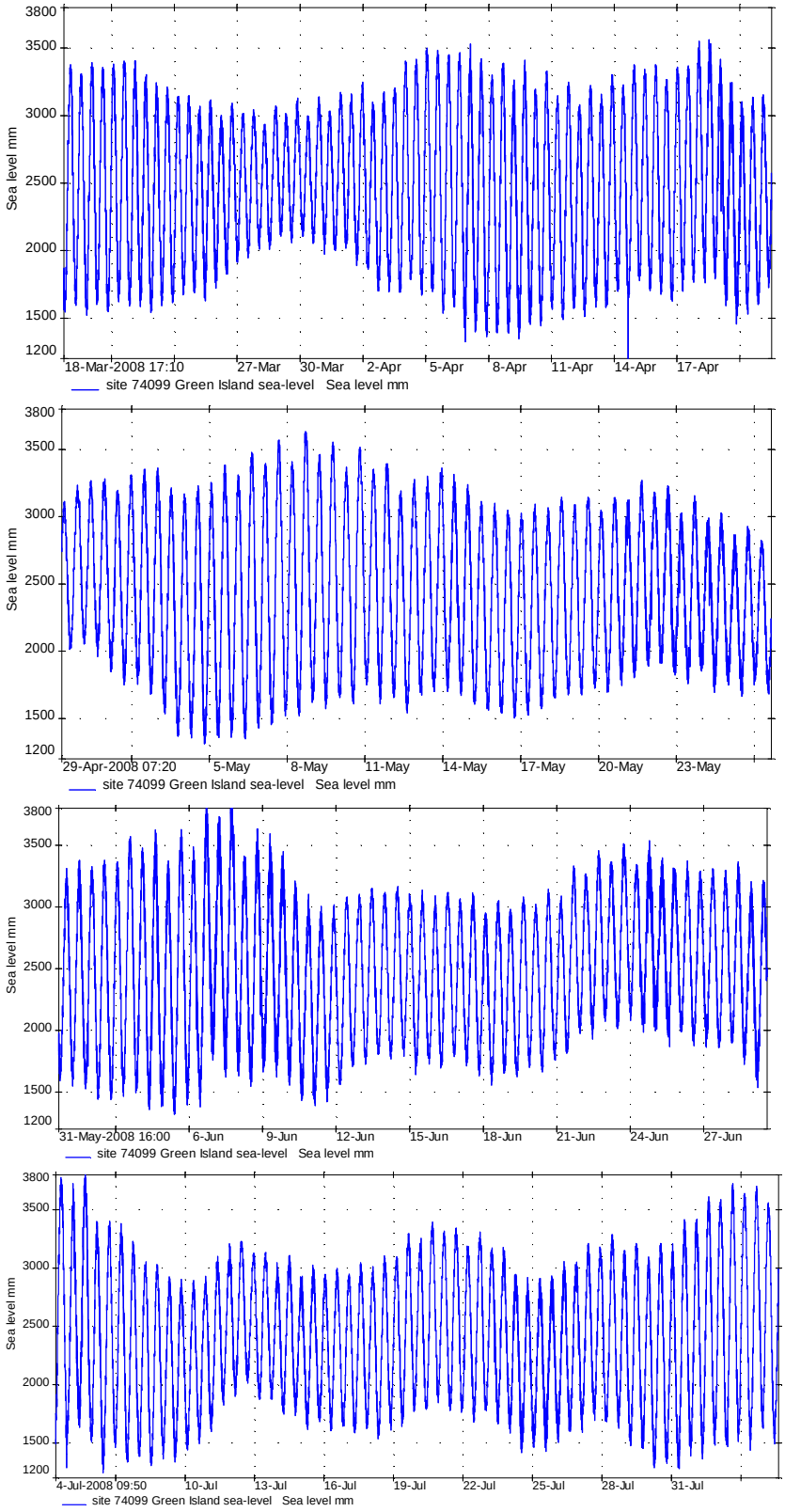

Figure 3.3: Sea levels recorded by the Green Island gauge split into the 4 field deployment periods.

4. Water-column properties

4.1 Temperature

Continuously logged temperature data were obtained at the surface (under the surface buoy) and at mid-depth for the inshore B1 & B2 ADCP mooring sites starting 21 April. Figure 4.1a shows the record, comparing the surface and mid-depth measurements, with a vertical line to show when the mooring system was moved from B1 (depth = 15.2 m) to B2 (depth = 15.3 m). The bottom temperatures recorded by the ADCP are shown in Figure 4.1b overlying the results previously shown in Figure 4.1a for moorings at B1 and B2.

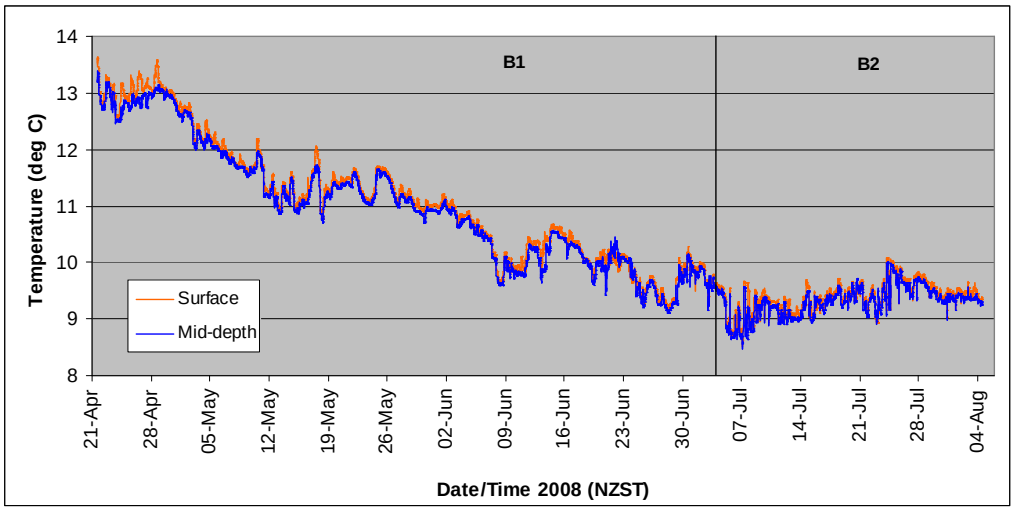

Figure 4.1a: Temperatures (°C) measured by HOBO Water Temperature Pro loggers (accuracy ±0.2°C) at the surface and mid-depth for the B1 mooring changing to the B2 mooring at 1200 hrs on 4-July.

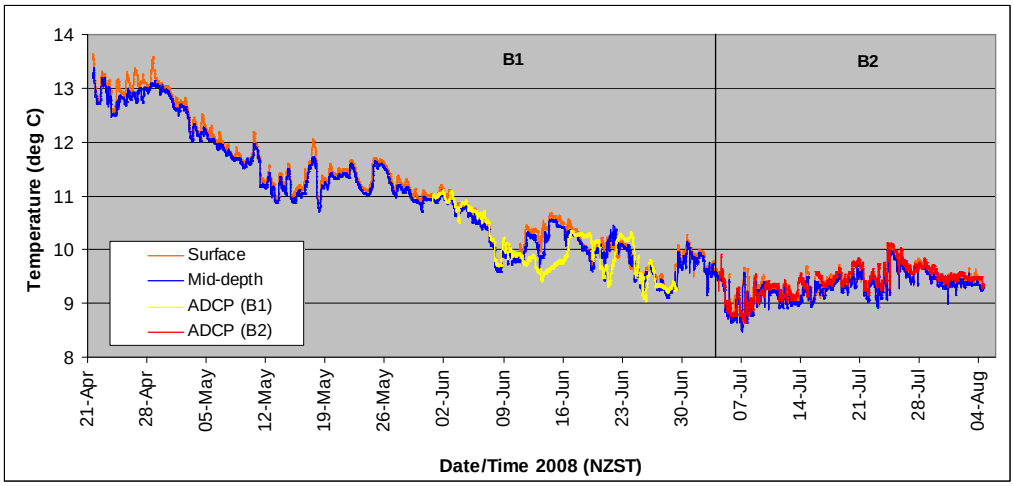

Figure 4.1b: Temperatures (°C) measured by HOBO Water Temperature Pro loggers at the surface and mid-depth for the B1 and B2 moorings (from Fig. 4.1a) supplemented by the ADCP temperature sensors at the seabed (15.2 m mean depth) for deployment B1 /3 and later at B2 (15.3 m mean depth).

Temperatures at the surface and mid-depth (approx. 7.5 m mean depth) followed a very similar pattern, with only a small offset in temperature, with the surface being warmer than the mid-depth of the water column by an average of 0.1°C for mooring B1 and an average offset of 0.08°C for the shorter B2 mooring.

Figure 4.1b shows the additional ADCP temperature records for B1 and B2 measured near the seabed. At the seabed, the temperature generally follows the trend measured higher in the water column, but there are periods when winds transport slightly warmer or cooler waters through the near-bed region at B1 (Blueskin Bay). However at B2 (Heyward Point) the entire water column was well mixed as shown on the right-hand side of Fig. 4.1b, with the difference of 0.1°C from surface to seabed being less than the accuracy of the temperature sensors (±0.2°C).

The generally small difference in the mean temperature down the water column means the density stratification due to temperature is only minor at the inshore sites with generally well-mixed conditions occurring. This pattern is punctuated by occurrences of upwelling or downwelling at the seabed in Blueskin Bay during strong south-westerlies and north-easterlies respectively (see Section 5).

Occasional peaks in the surface temperature record relative to the mid-depth temperature (e.g., at the start of the record in Fig. 4.1a) occur during calmer, sunny conditions when the surface layer heats up temporarily during the day.

Unfortunately, no temperature data were collected at the offshore A1 mooring, except for the 1-day CTD measurement on 27 May 2008. The temperature-depth profiles from the CTD for both the B1 and A1 moorings are compared in Figure 4.2. The total difference between the surface and bottom is < 0.1°C at site B1 and 0.15°C at site A1, with most of the temperature difference occurring at site A1 in the top 2 m. These measurements confirm that temperature stratification is not a significant factor to incorporate into the modelling of currents in the shelf area off Otago Heads (would be further out into the Southland Current) and also is unlikely to influence the dispersion of dredged sediment plumes during the disposal phase (given disposal from a dredge hopper would take place several metres below the surface). However, a depth-layered 3-dimensional model was still used in the modelling investigations to incorporate vertical effects of surface winds on currents (Bell et al. 2009).

The waters further offshore on the shelf were warmer by 0.4–0.45°C in the CTD profile (Figure 4.2) and match the pattern shown in the sea-surface satellite composite (Figure 4.3) that straddles the same period at the end of May. The decrease in nearshore temperatures for this time of year arises from the differential of the more stable temperatures of Subtropical waters in the Southland Current on the mid-continental shelf compared with the shallower nearshore waters, which cool more in winter due to cooler river and air temperatures and vice versa in summer.

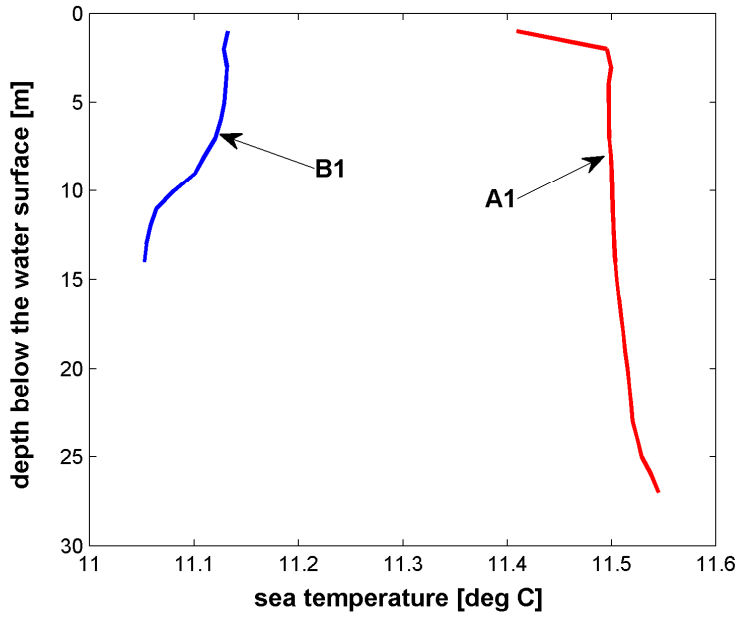

Figure 4.2: Temperature-depth profile measured at mooring sites B1 (inshore) and A1 (offshore) on 27-May-2008 between 1000 and 1040 hrs.

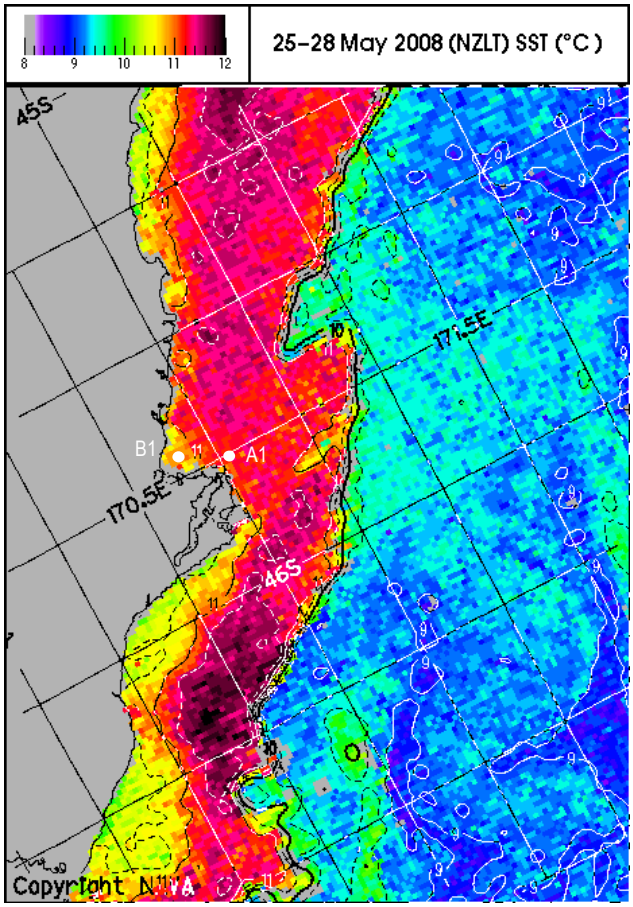

Figure 4.3: NIWA sea surface temperature (SST) map integrated over 25 to 28 May 2008 from NOAA satellite data, which coincides with the CTD profiling. The band of warmer waters in the mid-continental shelf (red colours) is indicative of Subtropical Water carried by the Southland Current. Mooring site locations A1 and B1 are annotated.

4.2 Salinity

Because the outflow from Otago Harbour and the Blueskin Bay area is not affected by large river flows, inshore waters are unlikely to exhibit any marked water density stratification in salinity (or proportion of freshwater) with depth down the water column. Salinity-depth profiles were obtained at the inshore B1 and offshore A1 moorings during CTD casts on 27 May 2008. Figure 4.4 shows that at the inshore site, salinity is uniform through the water column with little freshwater influence. Salinity reduces offshore with a more pronounced offset of nearly 0.3 between the surface and the bottom, which indicates the residual influence of the diluted Clutha River plume. As with temperature, most of the offset of salinity with depth occurs in the top 2–3 m, which is not likely to significantly influence the hydrodynamics in the inner-shelf region, nor the dispersion of the discharged sediment load from beneath a large dredge vessel with a substantial draught.

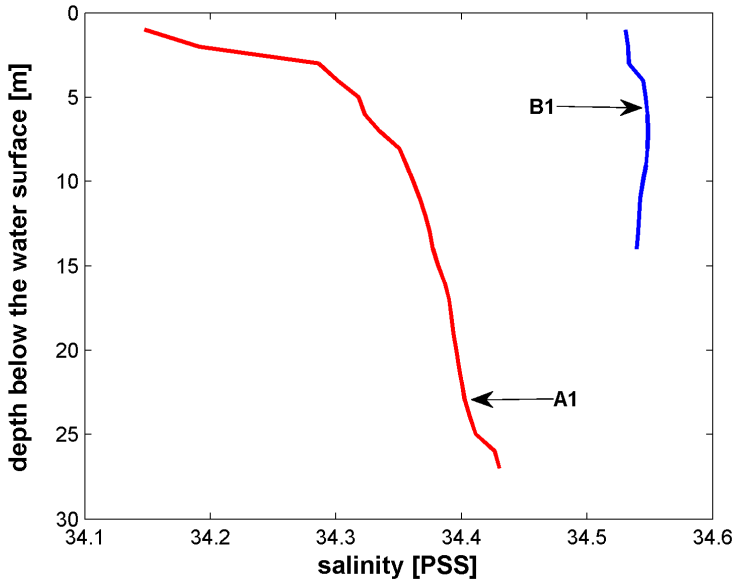

Figure 4.4: Salinity-depth profile measured at mooring sites B1 (inshore) and A1 (offshore) on 27-May-2008 between 1000 and 1040 hrs. [Note: salinity is measured in terms of the dimensionless Practical Salinity Scale or PSS].

5. Main results from the ADCP moorings

The results from each ADCP deployment are shown in this Section in the form of:

- Time series plots (currents at various heights, bottom temperature, depth).
- Time series of wind velocities from Taiaroa Head (uncorrected for the elevation of the weather station) to provide a visual cross-comparison with the measured currents and waves.
- Scatter plots of current velocity components *u* (east-west component, with east positive) and *v* (north-south component, with north positive), which show the overall distribution of current speeds in different directions.
- Progressive vector plots of the cumulative current-velocity run or net drift for various elevations above the bed. These are indicative of the net direction of suspended-sediment transport. While these plots show the net drift over several kilometres, they strictly only apply to water flows over the mooring site, because currents change spatially as different seafloor topography, coastline shape or oceanic currents are encountered further "downstream" from the mooring.
- Time series plots of derived wave statistics, described by the significant wave height H_s (which is the average of the top 33% of wave heights measured in a 20-minute period), peak period T_p in seconds (the averaged period between successive wave crests for those waves with the most energy as determined by the wave spectra), and peak wave direction D_p (which is the direction waves at the peak period are coming from) in degrees from True North.

5.1 Blueskin Bay (Site B1)

Two separate ADCP deployments were carried out at site B1, with details of the location and periods listed in Tables 2.1 to 2.2.

5.1.1 Deployment B1 /1

The set of time series plots for currents from deployment B1 /1 from 18 March to 03 April are shown in Figure 5.1 for 3 vertical heights above the seabed (Bin #1 at 1.5 m, Bin #8 at 8.5 m and Bin #12 at 12.5 m).

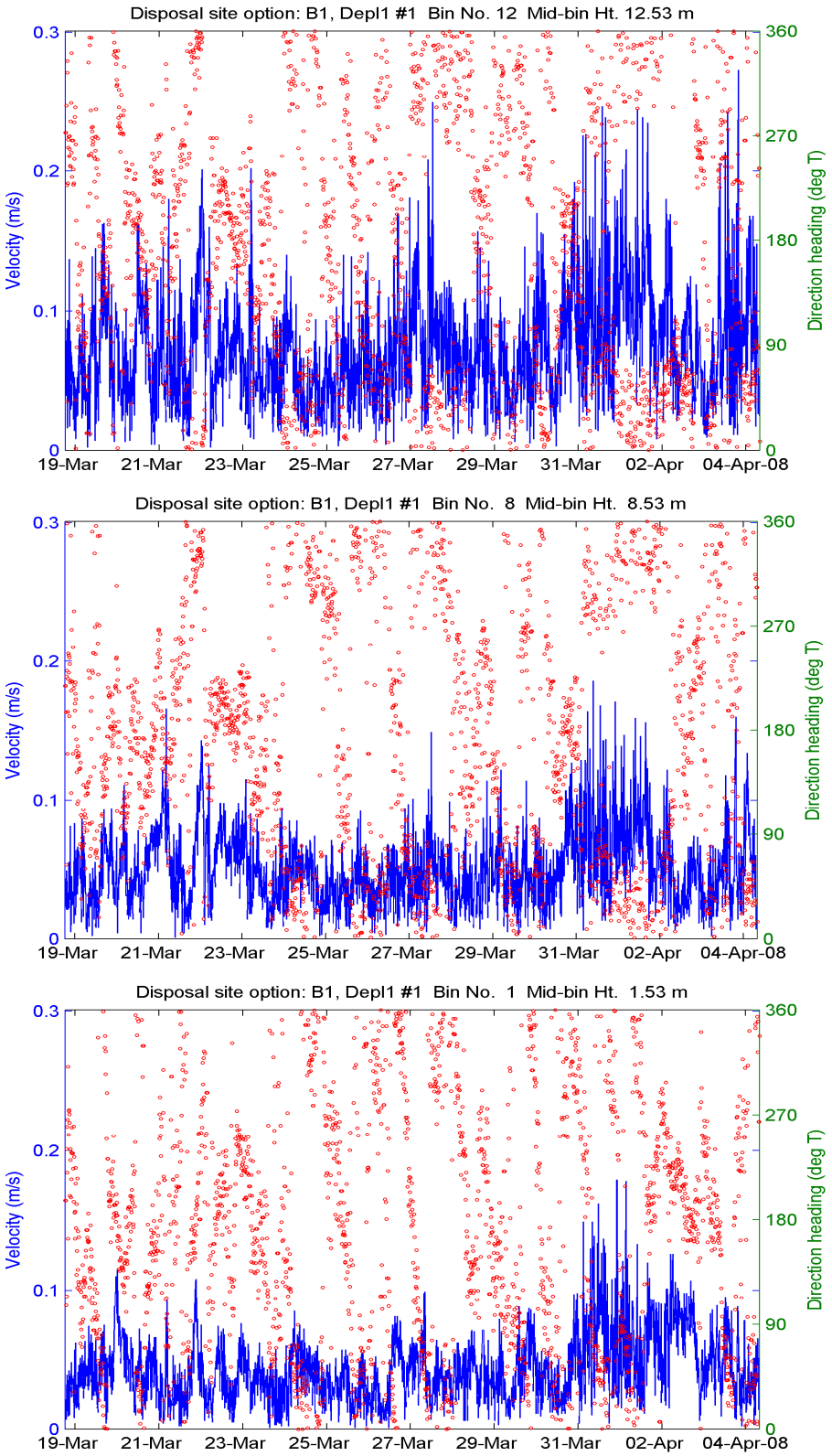

Figure 5.1: Current speeds (blue lines, left-hand scales) and directions (red dots, right-hand scale) at 3 different elevations above the bed for deployment B1 /1.

Near the seabed, the highest current speed of 0.18 m/s was reached on 31 March, following a 38-hour period of NE winds with speeds up to 10-11 m/s. Further up in the water column (top plot; Fig. 5.1), there were three main events including the aforementioned event, with a maximum current speed of 0.26 m/s briefly reached late on 03 April after a 30-hour period of strong SW winds with speeds up to 20 m/s.

Figure 5.2 shows the time series of water depth above the ADCP sensor (add 0.4 m for total water depth) and the near-bed sea temperature for deployment B1 /1.

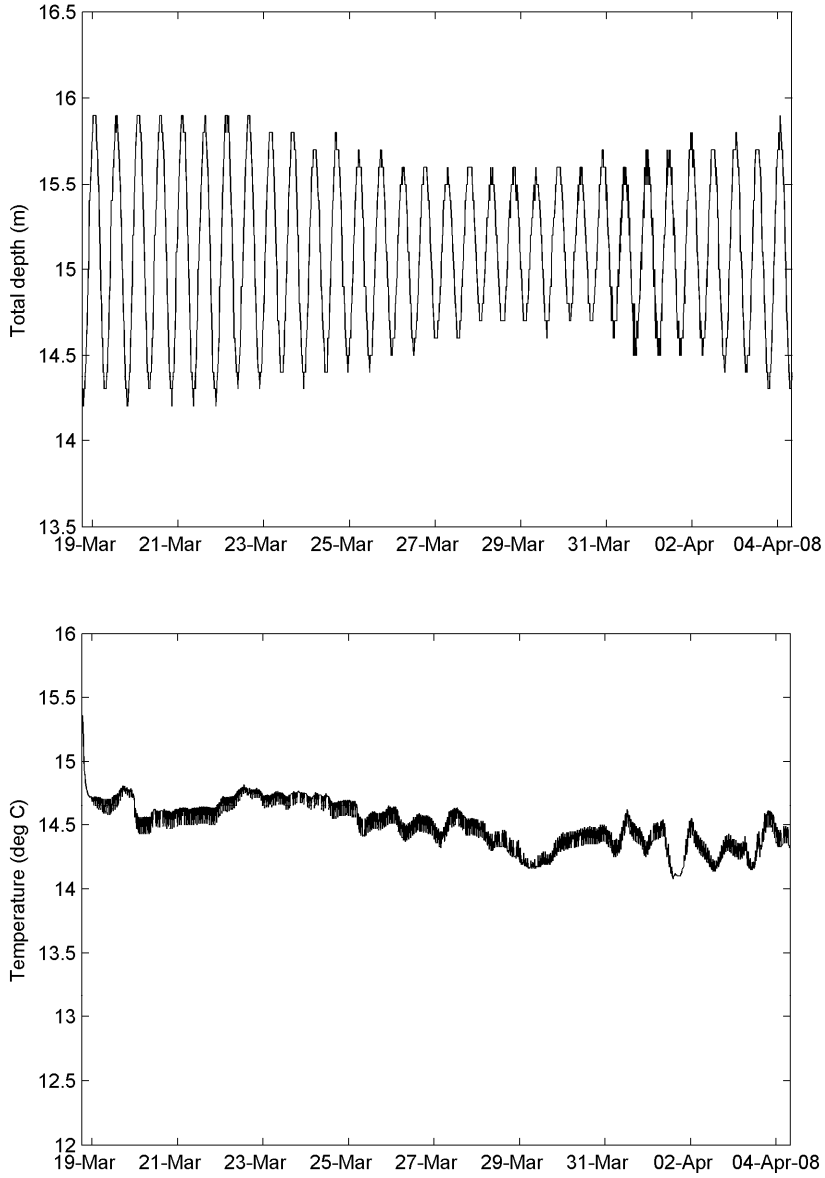

Figure 5.2: Water depth (TOP) and near-bed sea temperature (BOTTOM) for deployment B1 /1.

Winds that span the deployment period are shown in Figure 5.3.

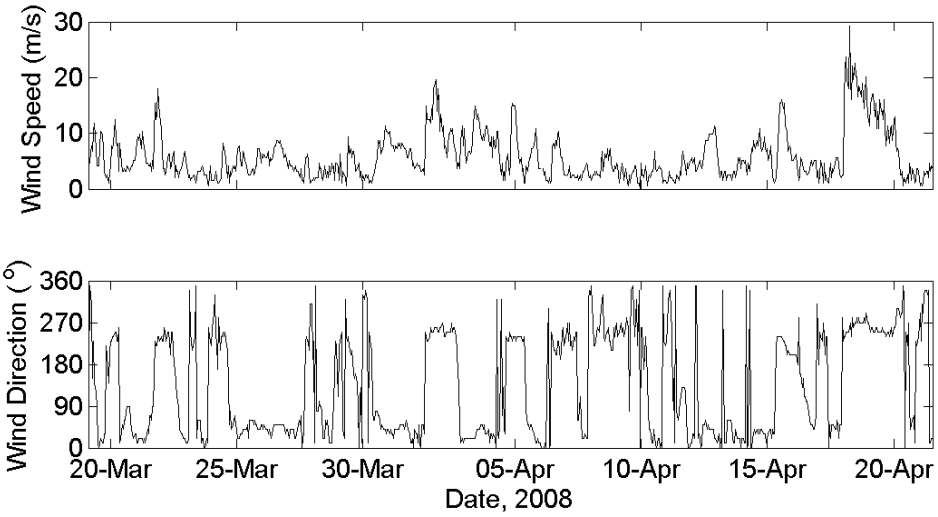

Figure 5.3: Wind speed (m/s) and direction (in meteorological convention "blowing from") at Taiaroa Head for deployment 1, noting B1 /1 terminated earlier on 4 April due to a malfunction.

Based on a tidal analysis over the 16.5 day record, the tides that could be resolved only explain 16% of the variability in the current velocities. The main twice-daily lunar tide (M_2) is quite small, peaking at 0.015 m/s along an axis oriented NNE and SSW. Wind is the dominant forcing for currents in Blueskin Bay as described by the results below.

The scatter plots of all velocities measured (irrespective of time) for two vertical bins near seabed and the upper water column are shown in Figure 5.4 along with the resulting principal component analysis. Each velocity is plotted according to its east-west (horizontal axis) and north-south (vertical axis) components of velocity (m/s). The major principal axis (thick line in Figure 5.4) is the orientation where the standard deviation or variability of the currents is a maximum, and its length is ±1 standard deviation (Table 5.1). The perpendicular minor principal axis is marked by the thin line based on the standard deviation listed in Table 5.1.

At both depths (Figure 5.4), the current velocities were distributed quite evenly in different compass directions, but they have a principal orientation (major axis) in the NE–SW direction that is influenced somewhat by the weak tidal currents to and for along a similar orientation. Current speeds are lower near the seabed (Bin #1), as expected.

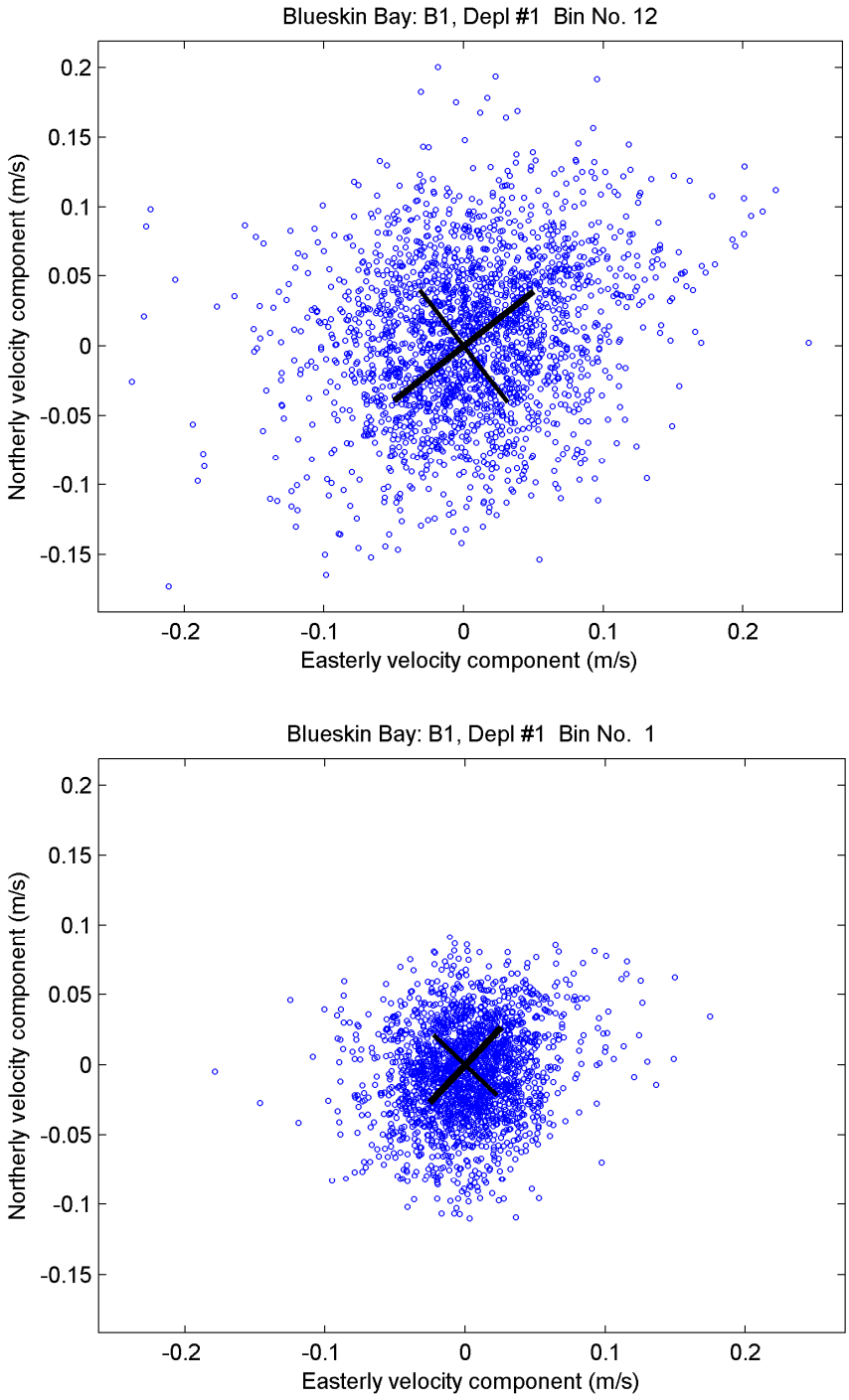

Figure 5.4: Scatter plots for currents at two bin heights from deployment B1 /1, based on the east-west current component (x-axis) and the north-south current component (y-axis). The thick line is the major principal axis, where the standard deviation is a maximum and the thinner line is the minor principal axis—both lines span ± 1 standard deviations in m/s.

Table 5.1: Summary of principal component analysis for currents during deployment B1 /1.

Bin No./depth	Major axis orientation (°True North)	Major axis std. dev (m/s)	Minor axis std. dev. (m/s)
12 (12.5 m)	52°	±0.063	±0.051
8 (8.5 m)	35°	±0.041	±0.038
1 (1.5 m)	44°	±0.037	±0.031

Unlike the scatter plots, progressive-vector or drift plots show the time sequence of currents. Figure 5.5 shows progressive vector plots for deployment B1 /1 at three bin heights in the water column. At all depths, the net or average current drift was small (<1 km/day) and the drift pattern involved a few circular meanders. The main difference was towards the end of the deployment (1-3 April) when a NE drift occurred nearer the surface caused by strong SW winds (i.e., down-wind drift) while near the seabed (Bin #1), the drift during this event was to the SW—the classic case of wind-driven upwelling onshore along the seabed during a strong surface wind blowing offshore. The net current drift velocities and directions are listed in Table 5.2, with the drift directions and speeds showing the influence of the strong SW wind event.

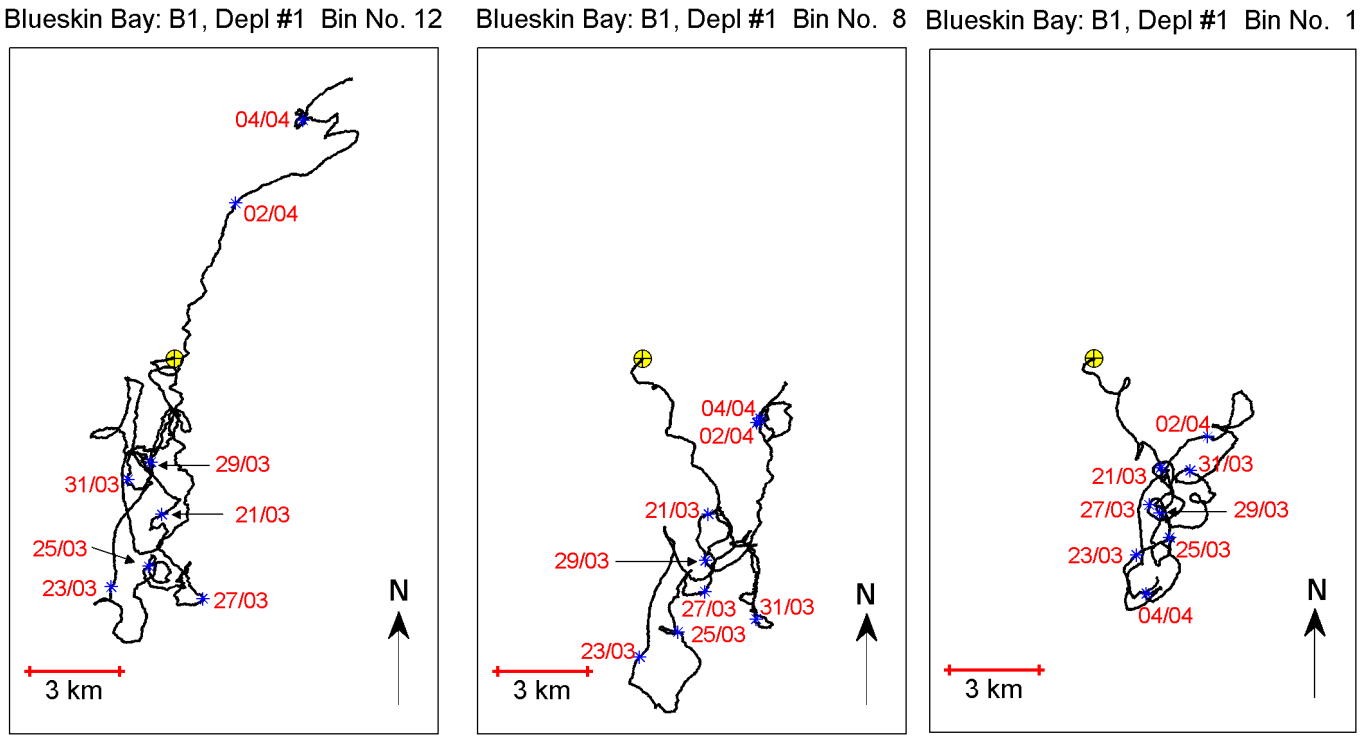

Figure 5.5: Progressive current drift at 3 depths from ADCP deployment B1 /1 starting 1840 18-Mar (yellow cross) through to 2340 04-Apr-2008 (total of 16.5 days). Every second day (0000 hrs) is marked by an asterisk and date-stamped in day/month format.

Table 5.2: Summary of the overall current drift during deployment B1 /1 (16.5 days).

Bin No./depth	Net drift velocity (m/s)	Net drift velocity (km/day)	Mean drift direction (°True North)
12 (12.5 m)	0.0077	0.66	32°
8 (8.5 m)	0.0033	0.29	99°
1 (1.5 m)	0.0053	0.46	164°

5.1.2 Deployment B1 /3

The set of time series plots for currents from deployment B1 /3 from 31 May to 29 June are shown in Figure 5.6 for 3 vertical elevations above the seabed (Bin #1 at 1.9 m, Bin #10 at 8.6 m and Bin #15 at 12.4 m). Note: these bin heights are different than the first deployment because a new ADCP was used with different vertical bin sizes (see Table 2.2).

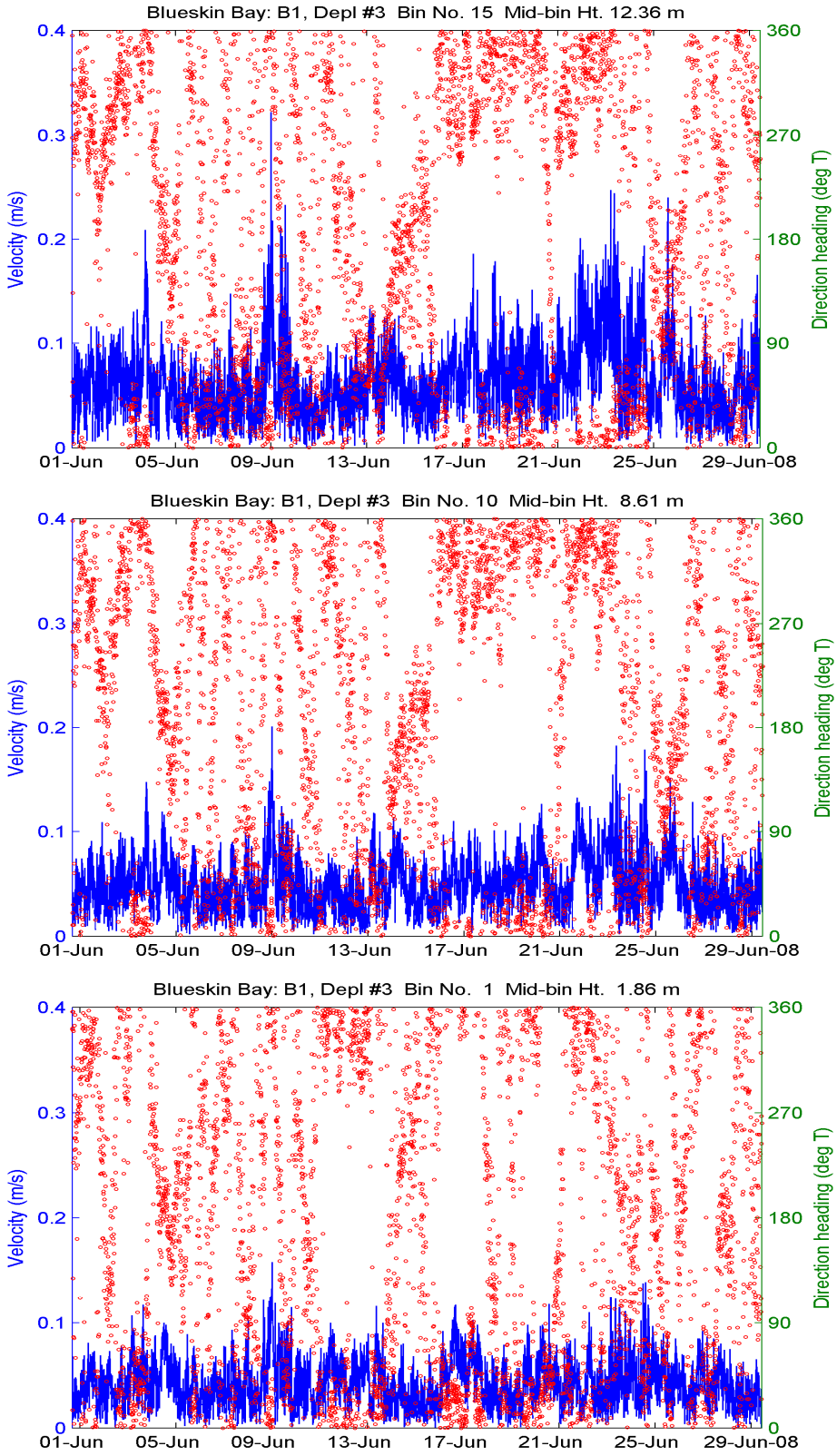

Figure 5.6: Current speeds (blue lines, left-hand scale) and directions (red dots, right-hand scale) at 3 different elevations above the bed for deployment B1 /3.

Near the seabed (Fig. 5.6), the highest current speeds of up to 0.16 m/s were reached early on 9 June, when winds of up to 28 m/s had blown for 2 days from the SW. Further up in the water column (12.4 m), the maximum current speed reached 0.32 m/s for the same event.

Figure 5.7 shows the time series of water depth above the ADCP sensor (add 0.4 m for total water depth) and the near-bed sea temperature for deployment B1 /3.

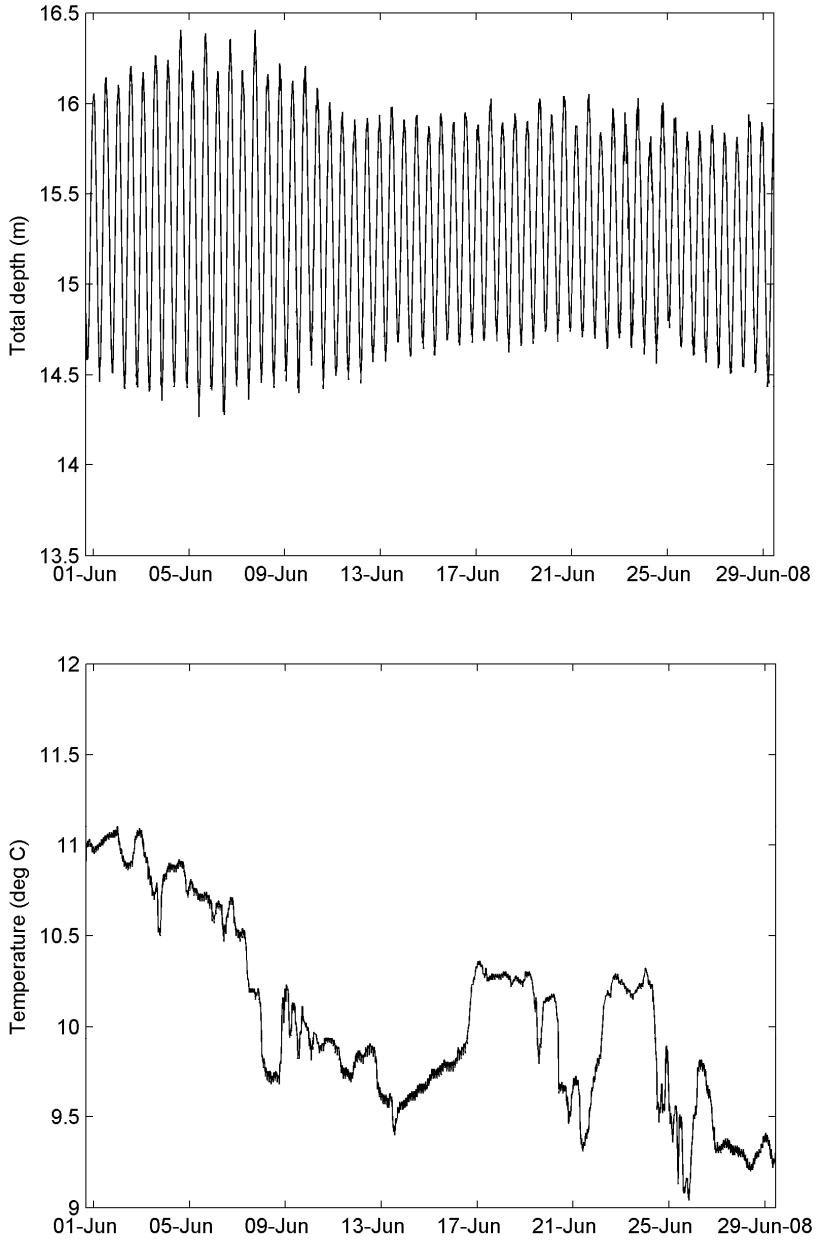

Figure 5.7: Water depth (TOP) and near-bed sea temperature (BOTTOM) for deployment B1 /3.

Winds that span the deployment period are shown in Figure 5.8.

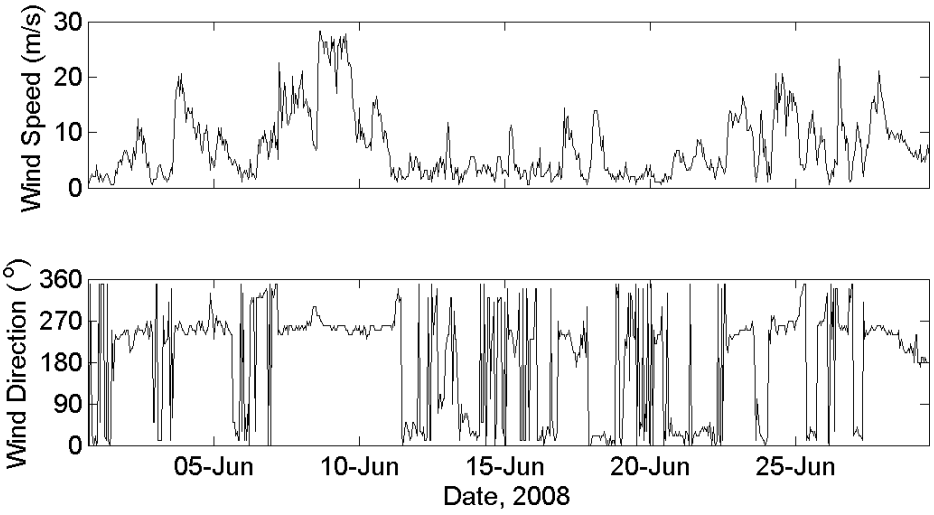

Figure 5.8: Wind speed (m/s) and direction (in meteorological convention "blowing from") at Taiaroa Head for deployment 3.

The scatter plots of all velocities measured for two vertical bins (near seabed and upper water column) are shown in Figure 5.9 with the resulting principal component analysis in Table 5.3.

At both depths (Figure 5.9), the currents were distributed in a similar pattern to deployment B1 /1 but with less scatter, especially in the upper water column (Bin #15). The preferred orientation (major axis) was also more northerly than the first deployment, lying in a NNE–SSW direction which is the same as the weak tidal current orientation. Current speeds are lower near the seabed (Bin #1), as expected.

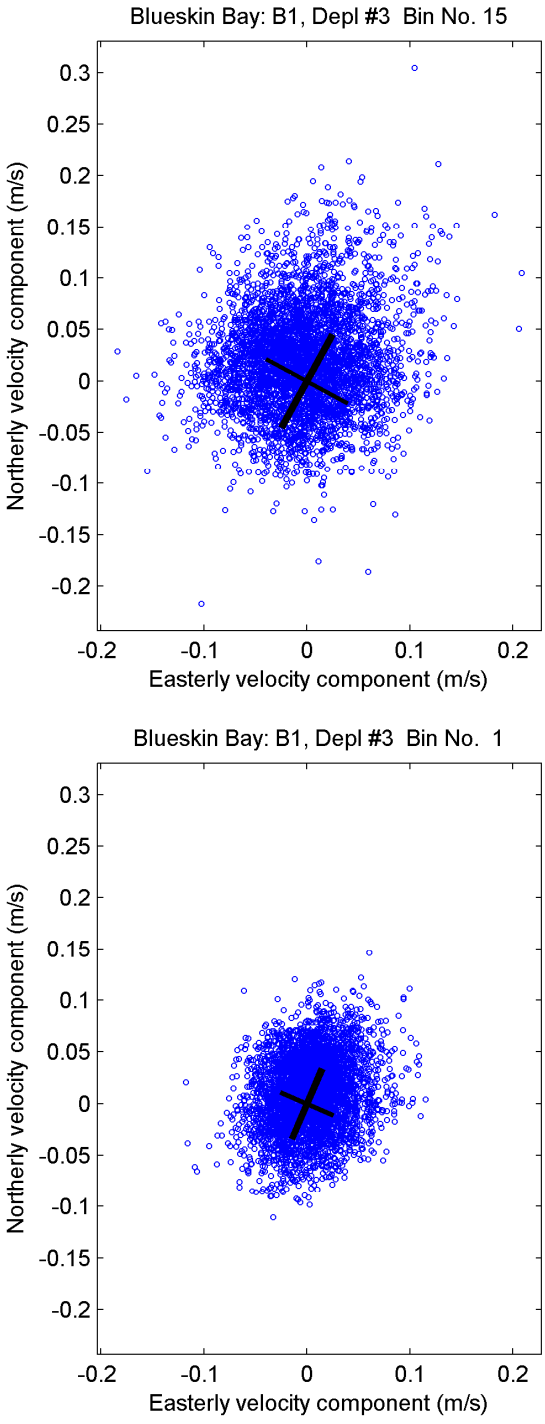

Figure 5.9: Scatter plots for currents at two bin heights from deployment B1 /3, based on the east-west current component (x-axis) and the north-south current component (y-axis). The thick line is the major principal axis, where the standard deviation is a maximum and the thinner line is the minor principal axis—both lines span ± 1 standard deviations in m/s.

Table 5.3: Summary of principal component analysis for currents during deployment B1 /3.

Bin No./depth	Major axis orientation (°True North)	Major axis std. dev (m/s)	Minor axis std. dev. (m/s)
15 (12.4 m)	29°	±0.051	±0.045
10 (8.6 m)	8°	±0.041	±0.034
1 (1.9 m)	23°	±0.037	±0.028

Figure 5.10 shows the progressive-vector plots for deployment B1 /3 at three bin heights in the water column. At all depths, the current drift was more consistently towards the northerly quarter compared to the first deployment (Figure 5.5), with much fewer meanders. This was mainly due to more frequent winds from the SW (Figure 5.8) than in the first deployment when NE winds were more frequent (Figure 5.4). The highest drift currents occurred during events when SW winds exceeded 10 m/s—one event on 7–9 June and three events over 10 m/s from 17–25 June. However, the latter period was probably influenced more by larger-scale shelf circulation as local winds were low at times during the 17–25 June period and also included a strong, but brief interlude of NE winds on 18 June which didn't alter the drift pattern. The overall net current drift velocities and directions are listed in Table 5.4.

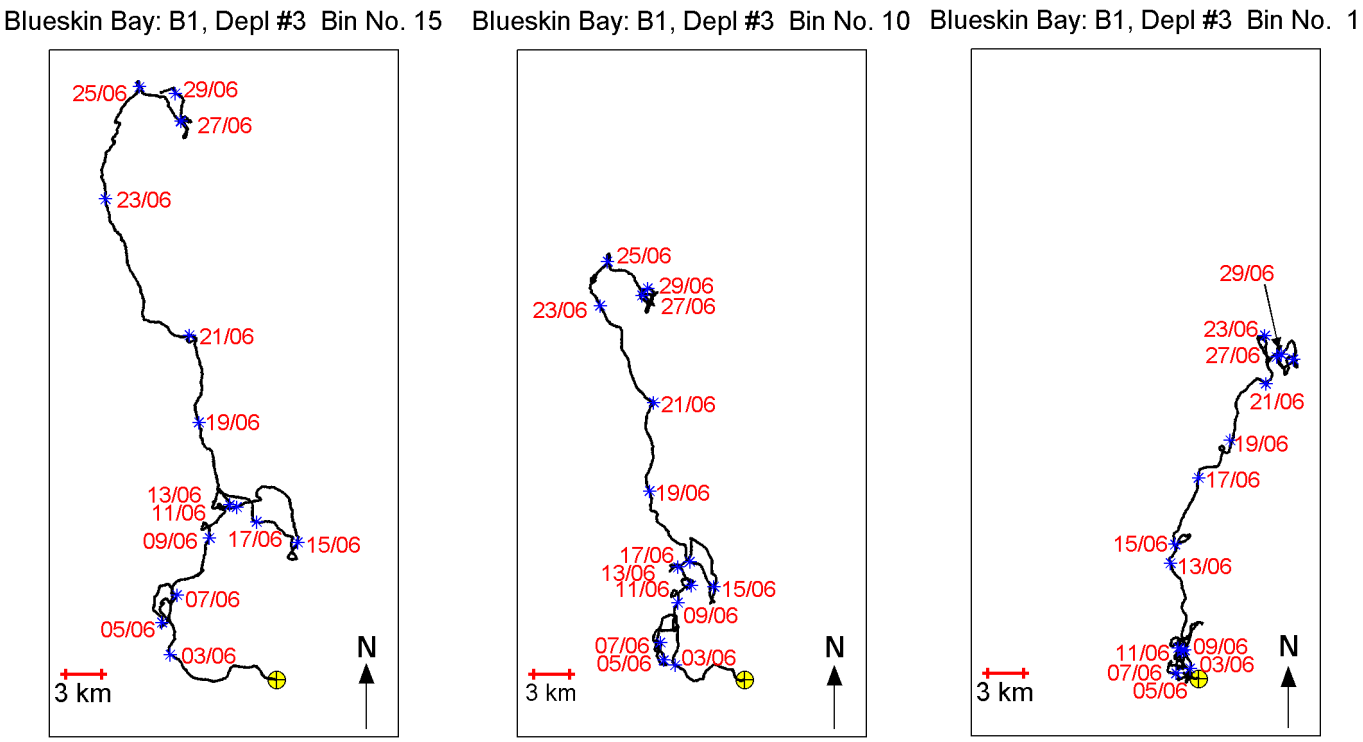

Figure 5.10: Progressive current drift at 3 depths from ADCP deployment B1 /3 starting 1600 31-May (yellow cross) through to 1040 29-Jun-2008 (total of 28.78 days). Every second day (0000 hrs) is marked by an asterisk and date-stamped in day/month format.

Table 5.4: Summary of the overall current drift during deployment B1 /3 (28.78 days).

Bin No./depth	Net drift velocity (m/s)	Net drift velocity (km/day)	Mean drift direction (°True North)
15 (12.4 m)	0.020	1.72	349°
10 (8.6 m)	0.013	1.15	345°
1 (1.9 m)	0.011	0.94	17°

5.2 Potential offshore disposal area (Site A1)

Four consecutive ADCP deployments were carried out at site A1, 2.2 nautical miles NE of Taiaroa Head and 1.4 nautical miles east of Landfall Tower that marks the approach channel. Details of the location and deployment periods are listed in Tables 2.1 to 2.2. Gaps of a few days occurred between deployments while the ADCP was downloaded and serviced on land and subsequently re-deployed when weather conditions were suitable. Besides measurements of currents, temperature and depth, wave summary statistics were also extracted for all four deployments.

5.2.1 Deployment A1 /1

The set of time series plots for currents from deployment A1 /1 from 18 March to 21 April are shown in Figure 5.11 for three vertical elevations above the seabed (Bin #1 at 1.9 m, Bin #14 at 11.6 m and Bin #28 at 22.1 m).

Near the seabed (Bin #1), the highest current speed of 0.34 m/s was reached on 19 April, following a 40-hour period of strong W to SW winds with speeds up to 29 m/s. Further up in the water column (top plot; Fig. 5.11), ignoring the obvious single spike early in the deployment, the maximum current speed of 0.56 m/s was reached on 30 March during NE winds with speeds up to 11 m/s.

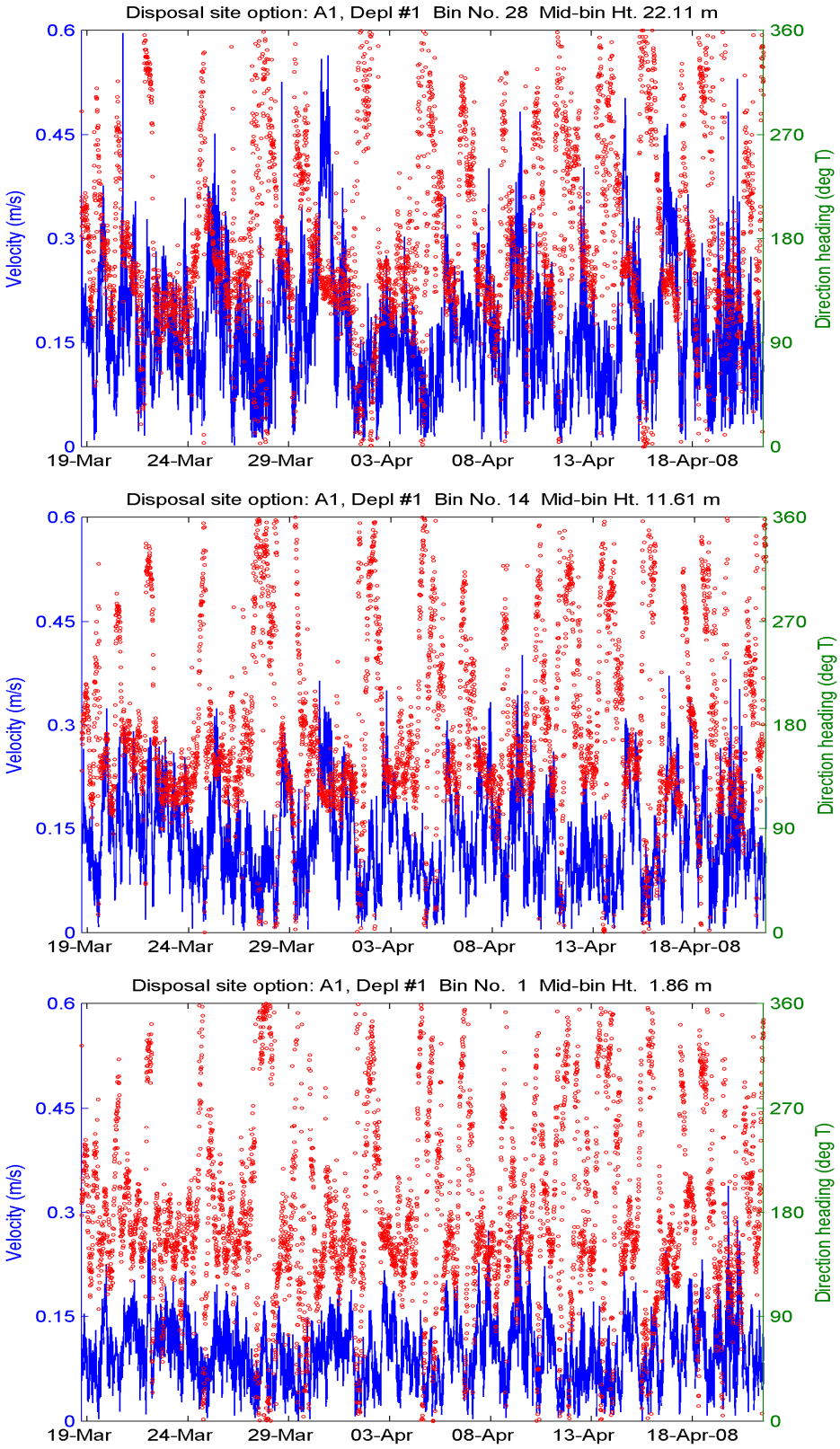

Figure 5.11: Current speeds (blue lines, left-hand scale) and directions (red dots, right-hand scale) at 3 different elevations above the bed for deployment A1 /1.

Figure 5.12 shows the time series of water depth above the ADCP sensor (add 0.4 m for total water depth) and the near-bed sea temperature for deployment A1 /1. Towards the end of the deployment, the rapid cooling from upwelling can be seen resulting from the strong SW event.

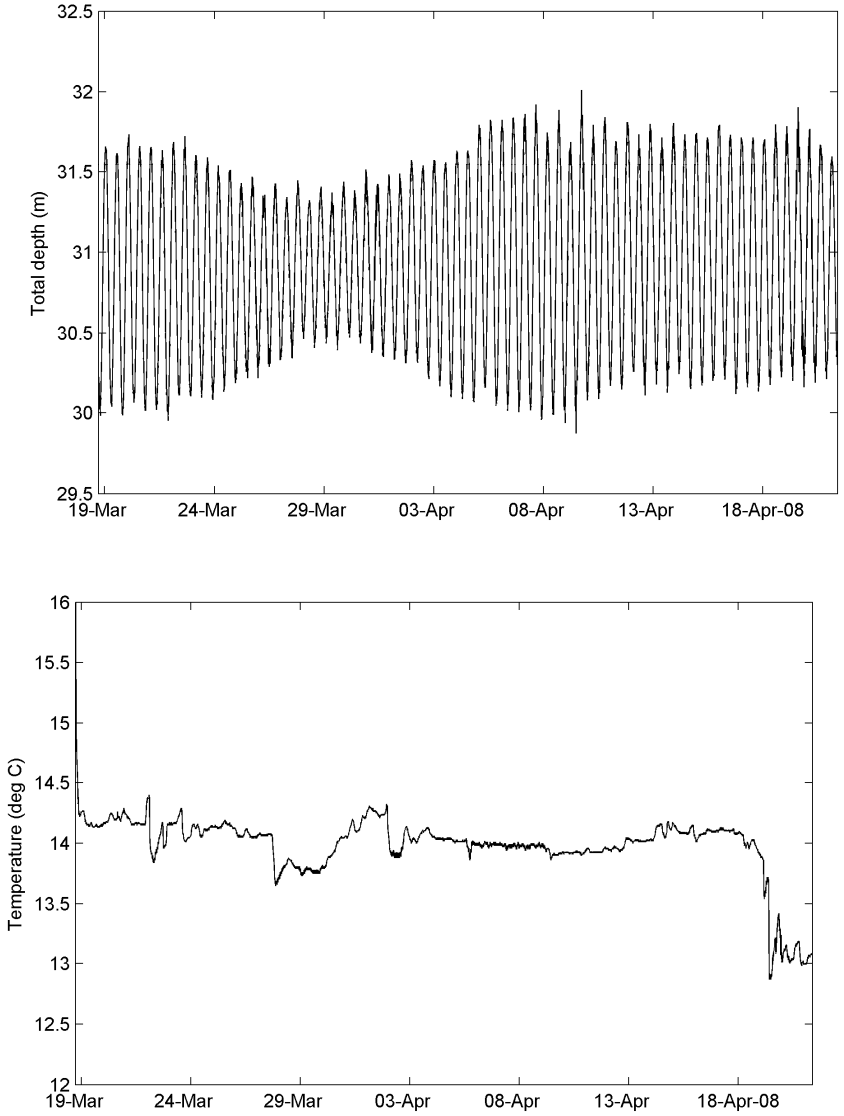

Figure 5.12: Water depth (TOP) and near-bed sea temperature (BOTTOM) for deployment A1 /1.

Winds that span the deployment period are shown in Figure 5.13, with the strongest event being the SW sequence on 18-19 April.

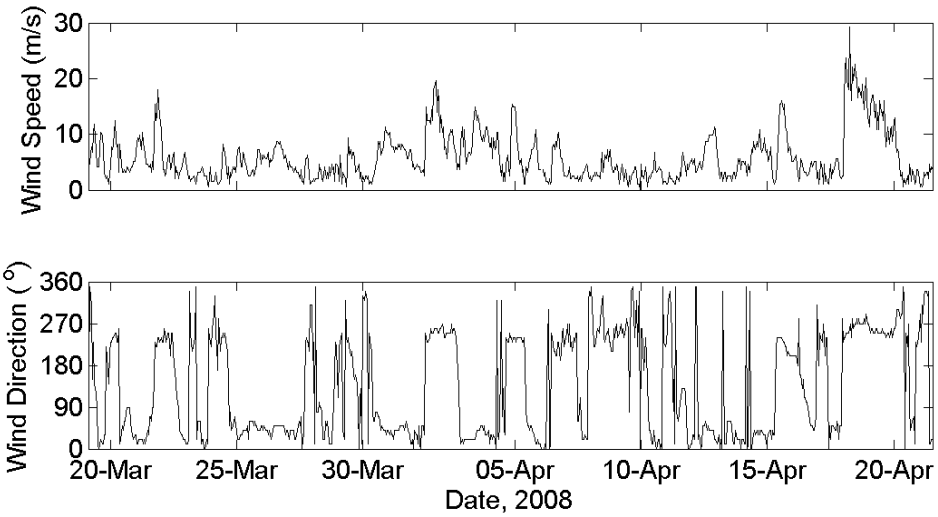

Figure 5.13: Wind speed (m/s) and direction (in meteorological convention "blowing from") at Taiaroa Head for deployment 1.

Based on a tidal analysis over the 33 day record from Bin #1 near the seabed, the tides that could be resolved explain 25% of the variability in the current velocities (14% in the north-south component and 37% in the east-west component). The main twice-daily lunar tide (M_2) current is modest, peaking at 0.05 m/s along an axis oriented WNW and ESE, which explains the higher percentage explained by tides in the east-west component. In Bin #14, the peak M_2 current was higher at 0.06 m/s, but tides explained less of the total variance (19%), with this trend continuing further up the water column. Overall, tides are a minor forcing for currents at site A1.

The scatter plots of all velocities measured for two vertical bins (near seabed and upper water column) are shown in Figure 5.14 with the resulting principal component analysis in Table 5.5.

At both depths (Figure 5.14), the currents are distributed reasonably evenly in different directions, but the larger currents have a preferred orientation (major axis) in the SE direction. As noted earlier, most of the currents to the east and west of the origin of the major and minor axes in Figure 5.14 are more influenced by the weak tidal currents which flow to and fro along an east-west alignment. Current speeds are lower near the seabed (Bin #1), as expected.

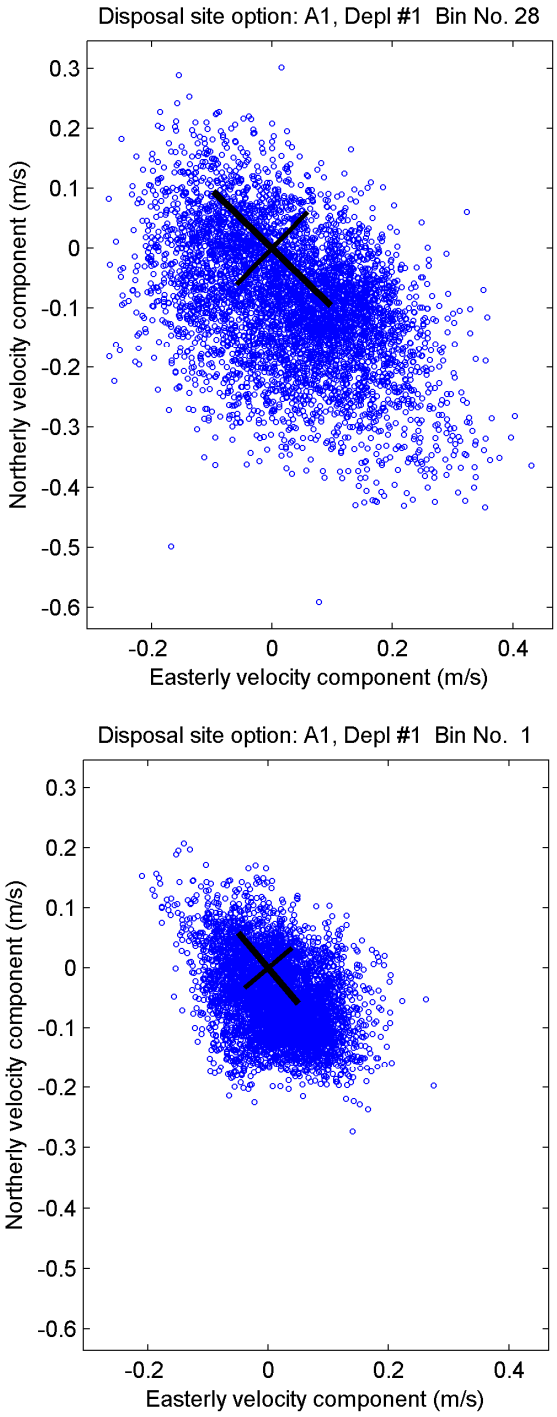

Figure 5.14: Scatter plots for currents at two bin heights from deployment A1 /1, based on the east-west current component (x-axis) and the north-south current component (y-axis). The thick line is the major principal axis, where the standard deviation is a maximum and the thinner line is the minor principal axis—both lines span ± 1 standard deviations in m/s.

Table 5.5: Summary of principal component analysis for currents during deployment A1 /1.

Bin No./depth	Major axis orientation (°True North)	Major axis std. dev (m/s)	Minor axis std. dev. (m/s)
28 (22.1 m)	134°	±0.136	±0.084
14 (11.6 m)	129°	±0.110	±0.059
1 (1.9 m)	140°	±0.077	±0.051

Figure 5.15 shows the progressive-vector plots for deployment A1 /1 at three bin heights in the water column. At all depths, the current drift was consistently towards the SSE, with only minor excursions in other directions e.g., the sawtooth pattern at times is due to the small tidal excursions. Near the seabed, the similar drift excursions between time-stamps indicates the residual current is consistent—possibly due to a headland eddy in conjunction with the Southland Current further offshore flowing north. The net current drift velocities and directions are listed in Table 5.6.

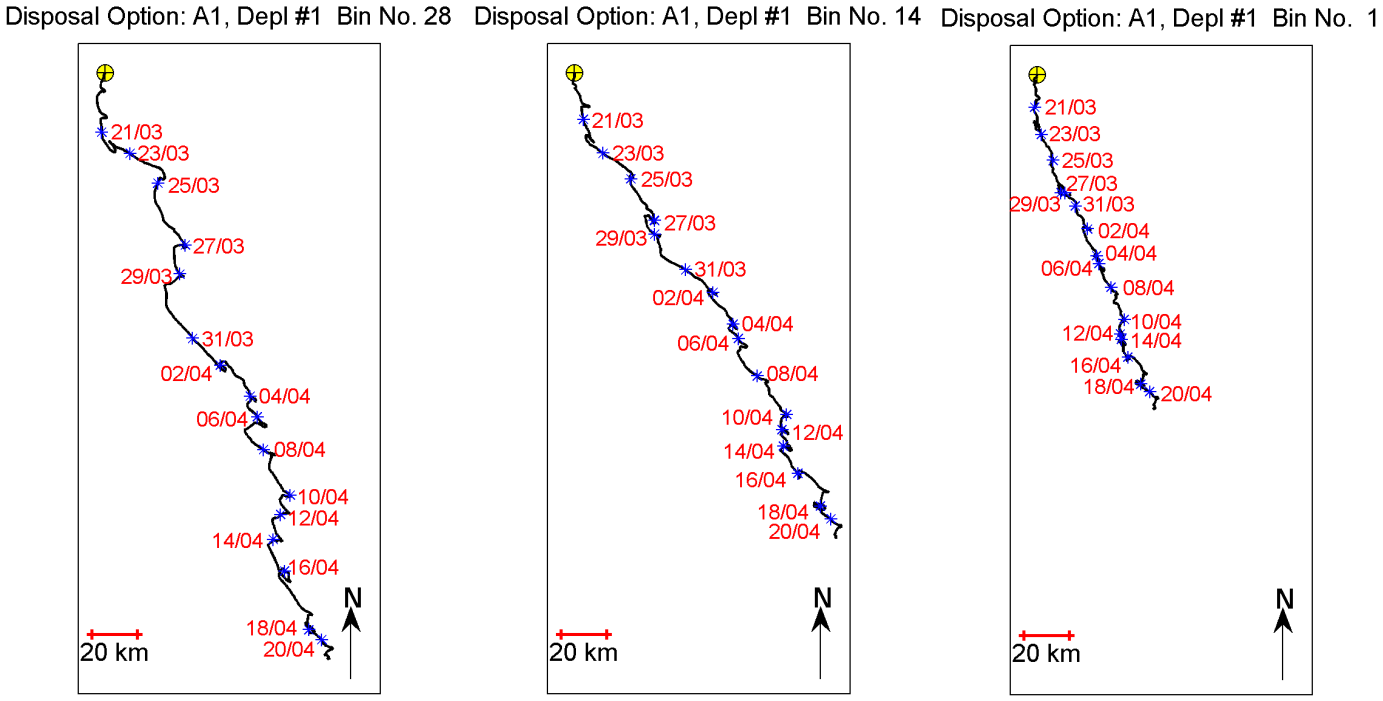

Figure 5.15: Progressive current drift at 3 depths from ADCP deployment A1 /1 starting 1710 18-Mar (yellow cross) through to 1230 21-Apr-2008 (total of 33.8 days). Every second day (0000 hrs) is marked by an asterisk and date-stamped in day/month format.

Table 5.6: Summary of the overall current drift during deployment A1 /1 (33.8 days).

Bin No./depth	Net drift velocity (m/s)	Net drift velocity (km/day)	Mean drift direction (°True North)
28 (22.1 m)	0.094	8.14	159°
14 (11.6 m)	0.080	6.92	151°
1 (1.9 m)	0.053	4.59	161°

Wave statistics were also extracted from the 20-minute bursts every hour during deployment A1 /1 and are shown in Figure 5.16. Wave direction is expressed in the same convention as winds—the direction from which waves arrive.

The highest significant wave height of 2.8 m was reached at 1600 h on 19 April 2008, with peak spectral periods of 12–14 seconds (swell) arriving from a SSE direction. The local winds at Taiaroa Head preceding this peak were strong south-westerlies.

Passages of NE winds cause a wind sea, evident from the lower spectral peak period (T_p < 10 sec) and the spectral-peak wave directions from the NE quarter (Figure 5.16).

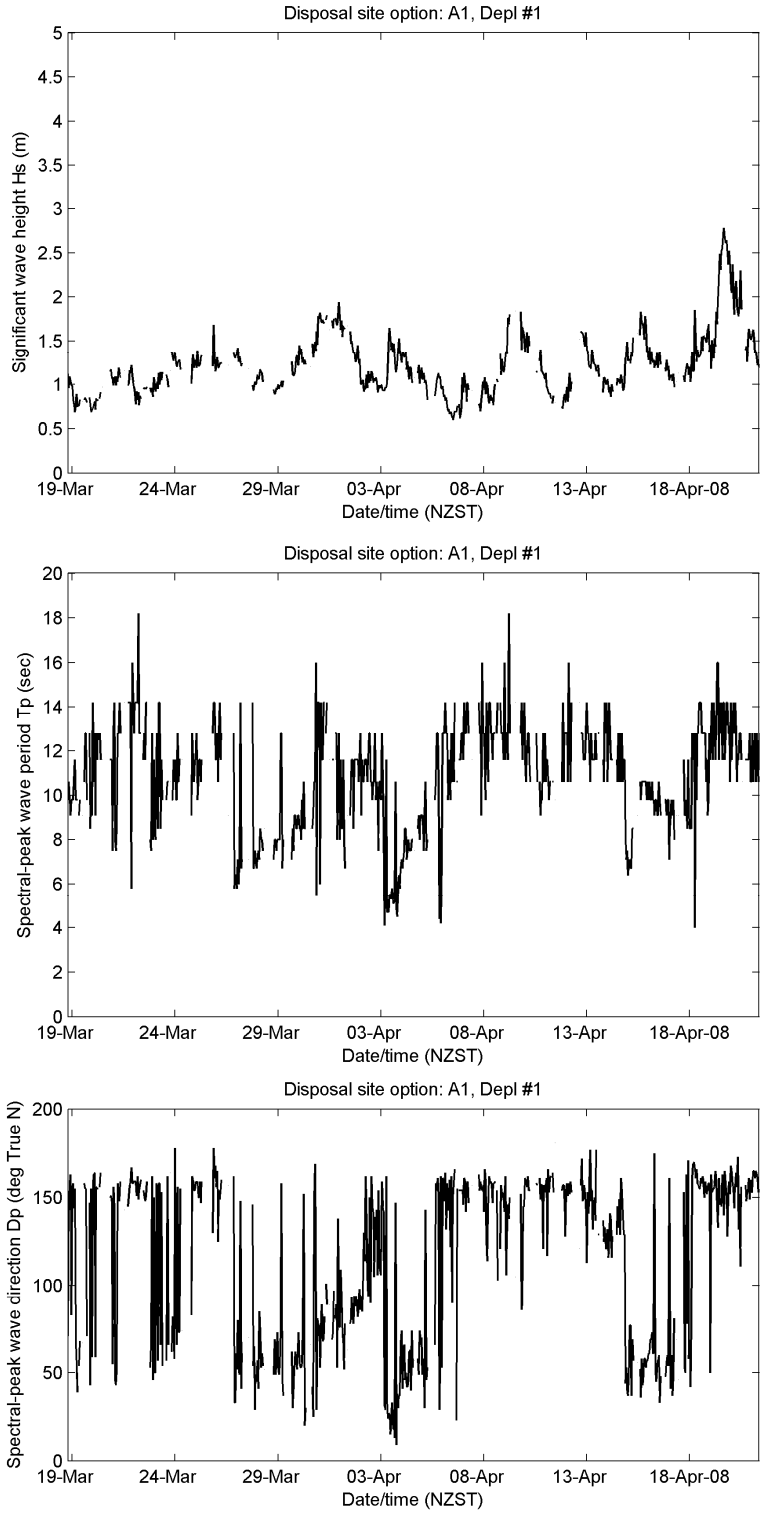

Figure 5.16: Wave statistics from deployment A1 /1: (top) significant wave height (H_s); (middle) spectral peak period (T_p); (bottom) spectral peak wave direction (D_p).

5.2.2 Deployment A1 /2

The set of time series plots for currents from deployment A1 /2 from 29 April to 26 May are shown in Figure 5.17 for three vertical elevations above the seabed (Bin #1 at 1.9 m, Bin #14 at 11.6 m and Bin #28 at 22.1 m).

The highest current speeds occurred on 23 May, ranging from 0.28 m/s near the seabed (Bin #1), to 0.46 m/s in Bin #28, following a day of SSW to SW winds with speeds up to 12 m/s.

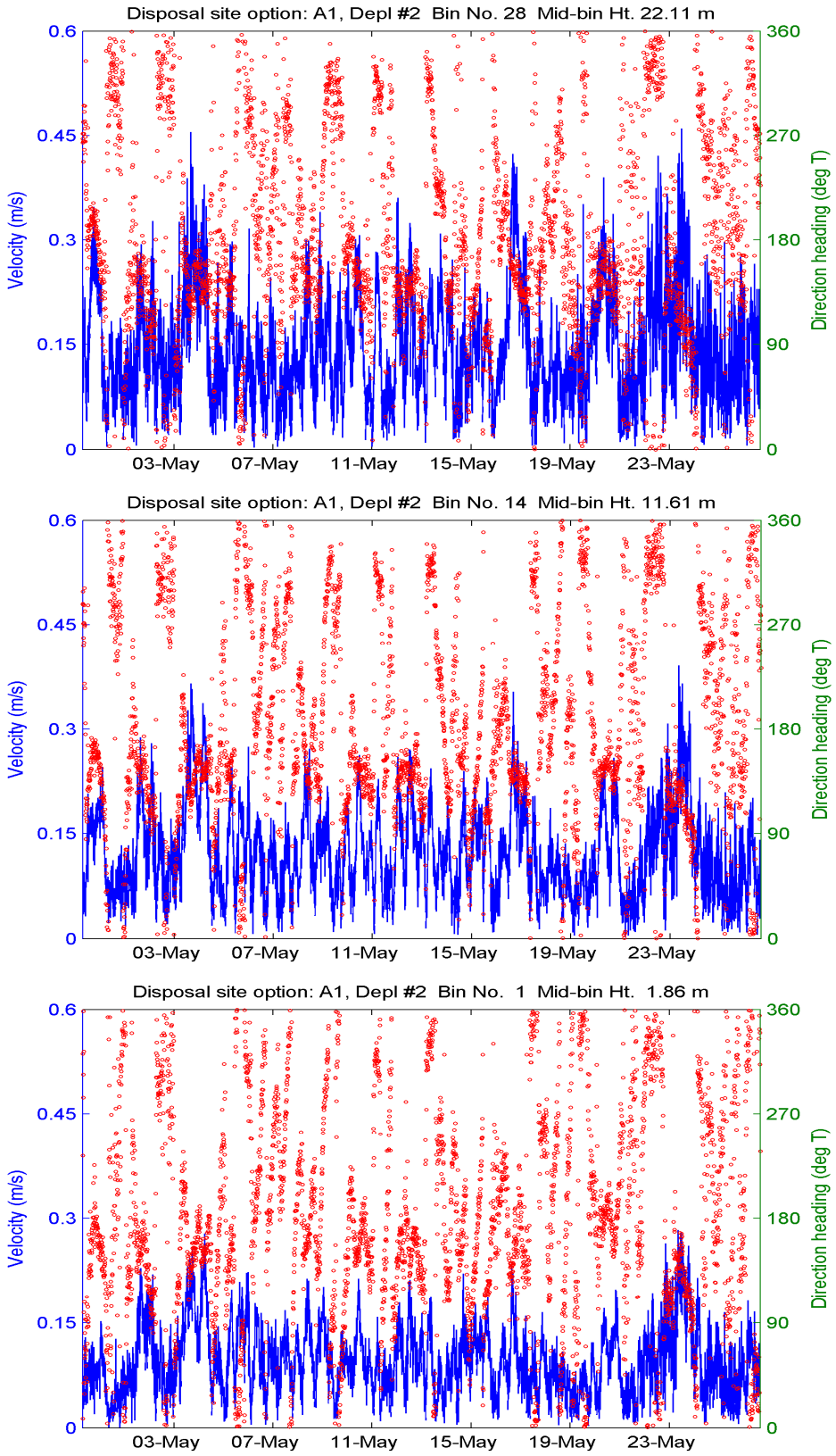

Figure 5.17: Current speeds (blue lines, left-hand scale) and directions (red dots, right-hand scale) at 3 different elevations above the bed for deployment A1 /2.

Figure 5.18 shows the time series of water depth above the ADCP sensor (add 0.4 m for total water depth) and the near-bed sea temperature for deployment A1 /2. Water temperature near the seabed progressively decreased over this autumn period as expected, but increased substantially on 20–21 May arising from downwelling produced by strong NE winds up to 15 m/s.

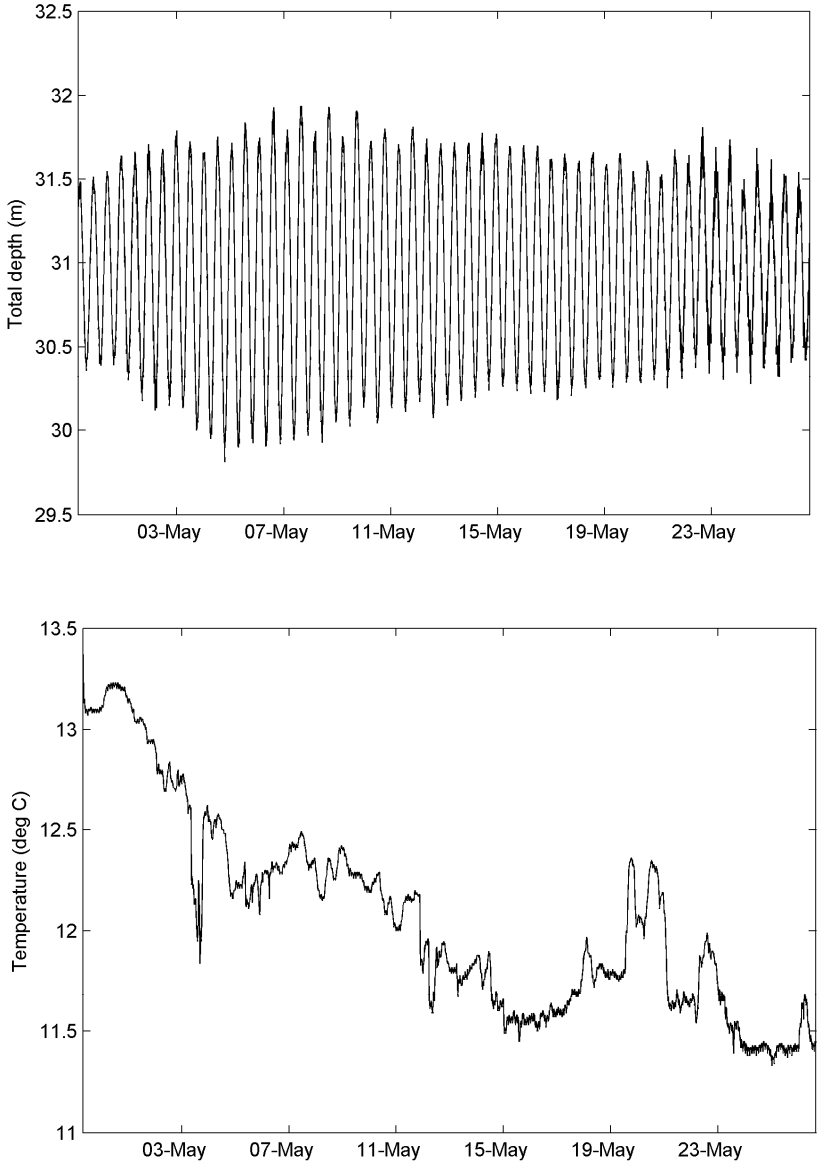

Figure 5.18: Water depth (TOP) and near-bed sea temperature (BOTTOM) for deployment A1 /2.

Winds that span the deployment period are shown in Figure 5.19, with the strongest wind speed of 20 m/s occurring on early on 1 May during a sustained SW wind sequence through to 4 May.

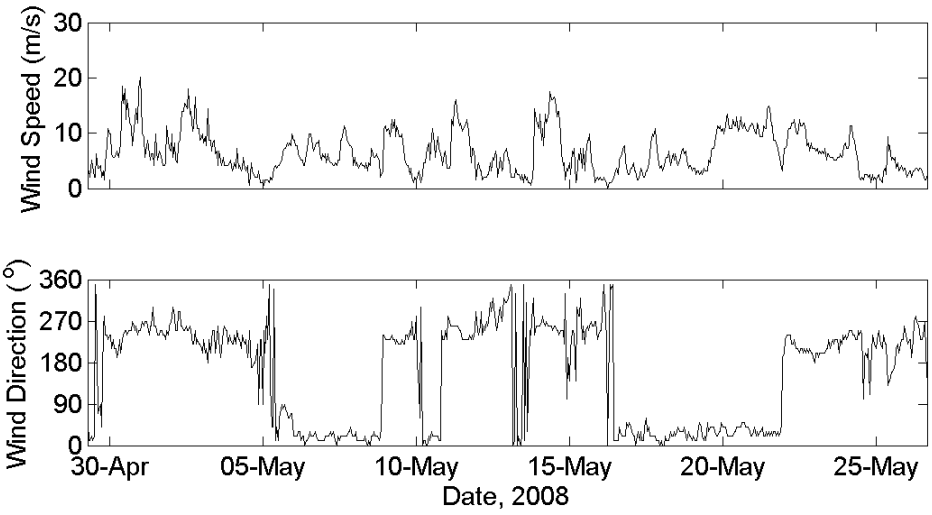

Figure 5.19: Wind speed (m/s) and direction (in meteorological convention "blowing from") at Taiaroa Head for deployment 2.

The scatter plots of all velocities measured for two vertical bins (near seabed and upper water column) are shown in Figure 5.20 with the resulting principal component analysis in Table 5.7.

At both depths (Figure 5.20), the currents are distributed reasonably evenly in different directions, but the larger currents have a preferred orientation (major axis) in the same SE direction as demonstrated in deployment 1. The principal (major) current directions and standard deviations listed in Table 5.7 are quite similar and consistent with the results from deployment 1 (Table 5.5), which supports the existence of a persistent eddy off the Otago Heads.

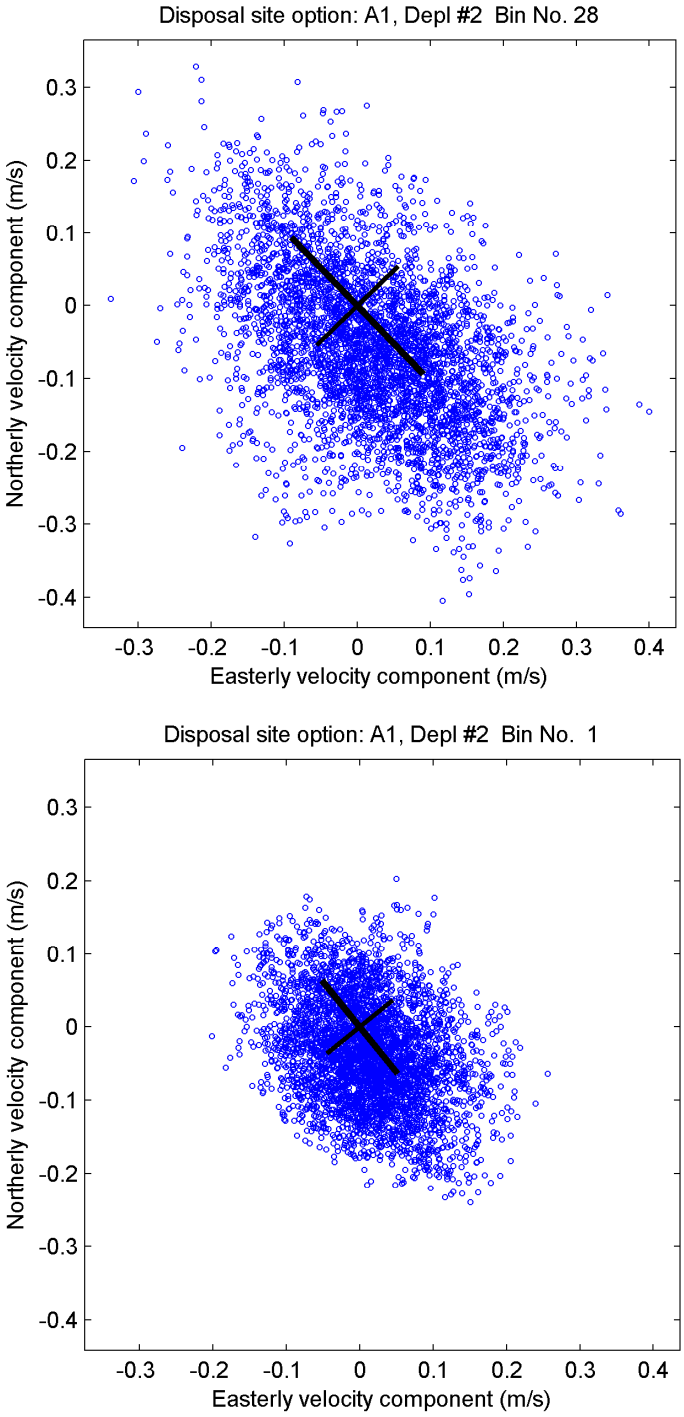

Figure 5.20: Scatter plots for currents at two bin heights from deployment A1 /2, based on the east-west current component (x-axis) and the north-south current component (y-axis). The thick line is the major principal axis, where the standard deviation is a maximum and the thinner line is the minor principal axis—both lines span ± 1 standard deviations in m/s.

Table 5.7: Summary of principal component analysis for currents during deployment A1 /2.

Bin No./depth	Major axis orientation (°True North)	Major axis std. dev (m/s)	Minor axis std. dev. (m/s)
28 (22.1 m)	136°	±0.130	±0.077
14 (11.6 m)	133°	±0.112	±0.059
1 (1.9 m)	141°	±0.081	±0.058

Figure 5.21 shows the progressive-vector plots for deployment A1 /2 at three bin heights in the water column. At all depths, the current drift was again consistently towards the SSE, with only minor excursions in other directions e.g., the sawtooth pattern at times is due to the small tidal excursions. Near the seabed, the similar drift excursions between time-stamps indicates the residual current is consistent. The net current drift velocities and directions are listed in Table 5.8. The net drift velocities were considerably lower than the previous deployment (Table 5.6), but the mean drift directions were very similar. These similarities and consistencies support the presence of a headland eddy in conjunction with the Southland Current flowing to the north.

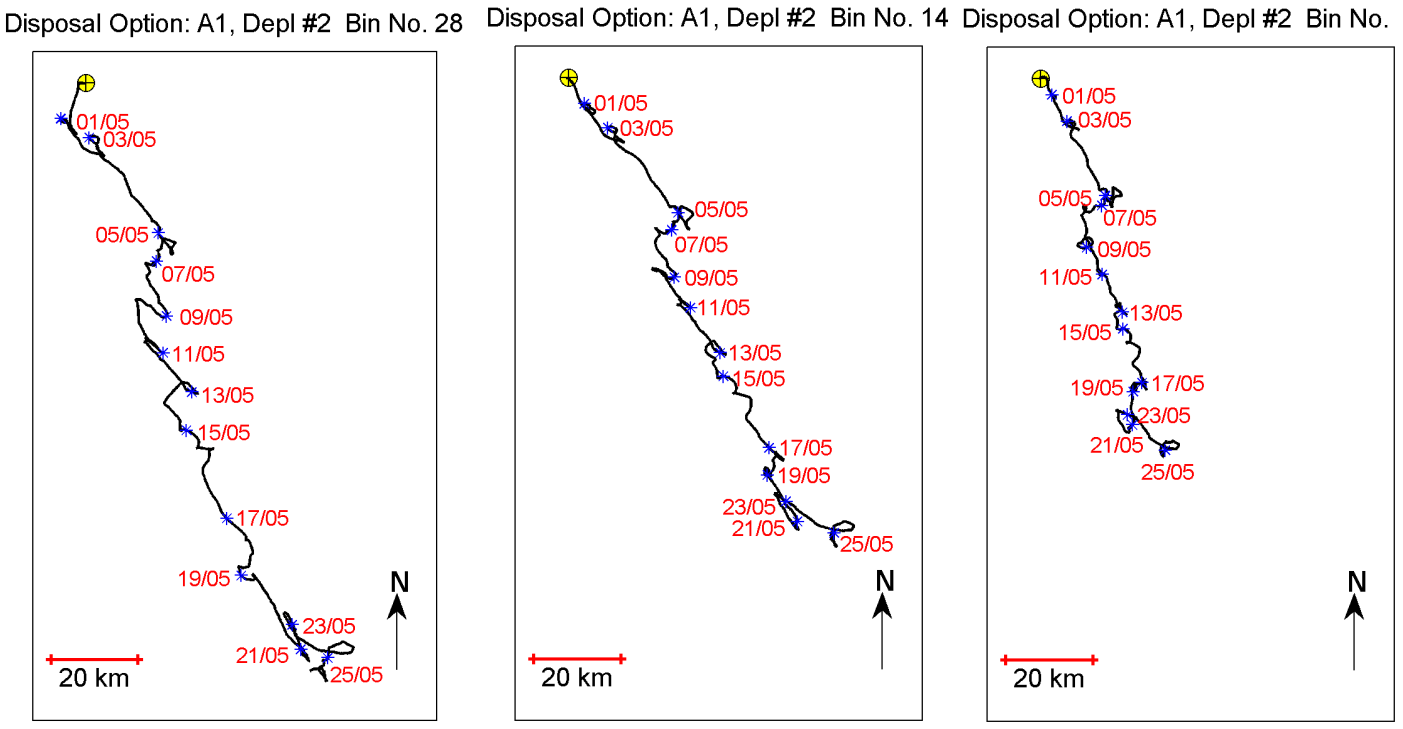

Figure 5.21: Progressive current drift at 3 depths from ADCP deployment A1 /2 starting 0720 29-April (yellow cross) through to 1600 26-May-2008 (27.36 days). Every second day (0000 hrs) is marked by an asterisk and date-stamped in day/month format.

Table 5.8: Summary of the overall current drift during deployment A1 /2 (27.36 days).

Bin No./depth	Net drift velocity (m/s)	Net drift velocity (km/day)	Mean drift direction (°True North)
28 (22.1 m)	0.062	5.31	159°
14 (11.6 m)	0.051	4.40	150°
1 (1.9 m)	0.037	3.21	161°

Wave statistics were also extracted from the 20-minute bursts every 2 hours during deployment A1 /2 and are shown in Figure 5.22. Wave direction is expressed in the same convention as winds—the direction from which waves arrive from.

The highest significant wave height of 3.0 m was reached at 1800 h on 22 May 2008, with peak spectral periods of 11–12 seconds (swell) arriving from a SSE direction. The local winds at Taiaroa Head preceding this peak were moderate SSW winds.

A period of moderate NE winds from 18–21 May produced a steadily rising wind sea from spectral peak periods of 6 to 8 seconds (Figure 5.22).

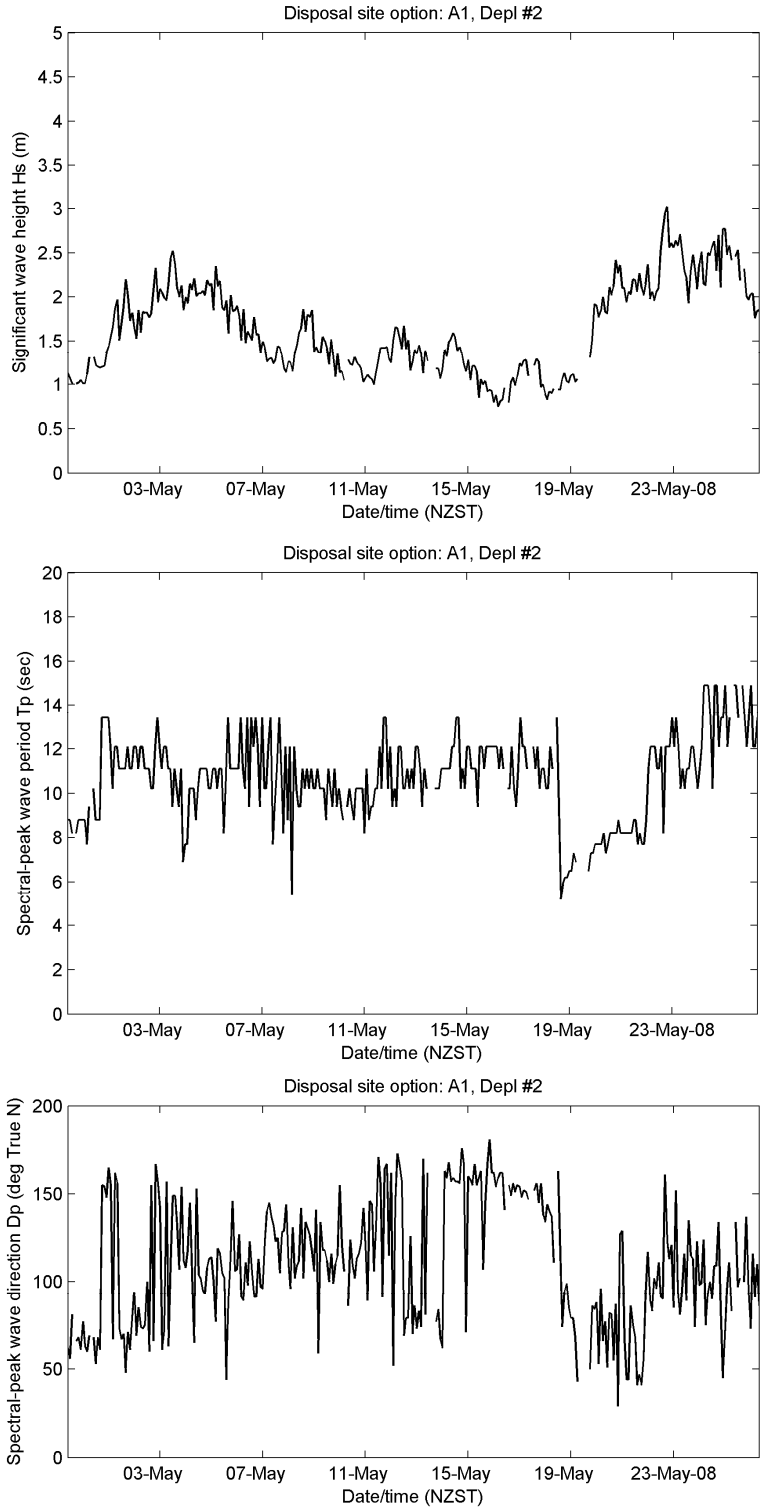

Figure 5.22: Wave statistics from deployment A1 /2: (top) significant wave height (H_s); (middle) spectral peak period (T_p); (bottom) spectral peak wave direction (D_p).

5.2.3 Deployment A1 /3

The set of time series plots for currents from deployment A1 /3 from 31 May to 29 June are shown in Figure 5.23 for three vertical elevations above the seabed (Bin #1 at 1.9 m, Bin #14 at 11.6 m and Bin #28 at 22.1 m).

The highest current speed near the seabed (Bin #1) reached 0.36 m/s late on 9 June following a period of strong WSW winds up to 28 m/s. The maximum current in Bin #14 of 0.44 m/s occurred 15 hours later. In the upper bin (Bin #28), the maximum current was measured on 18 June at 0.54 m/s, after an 8-hour period of winds from the NNE up to 14 m/s.

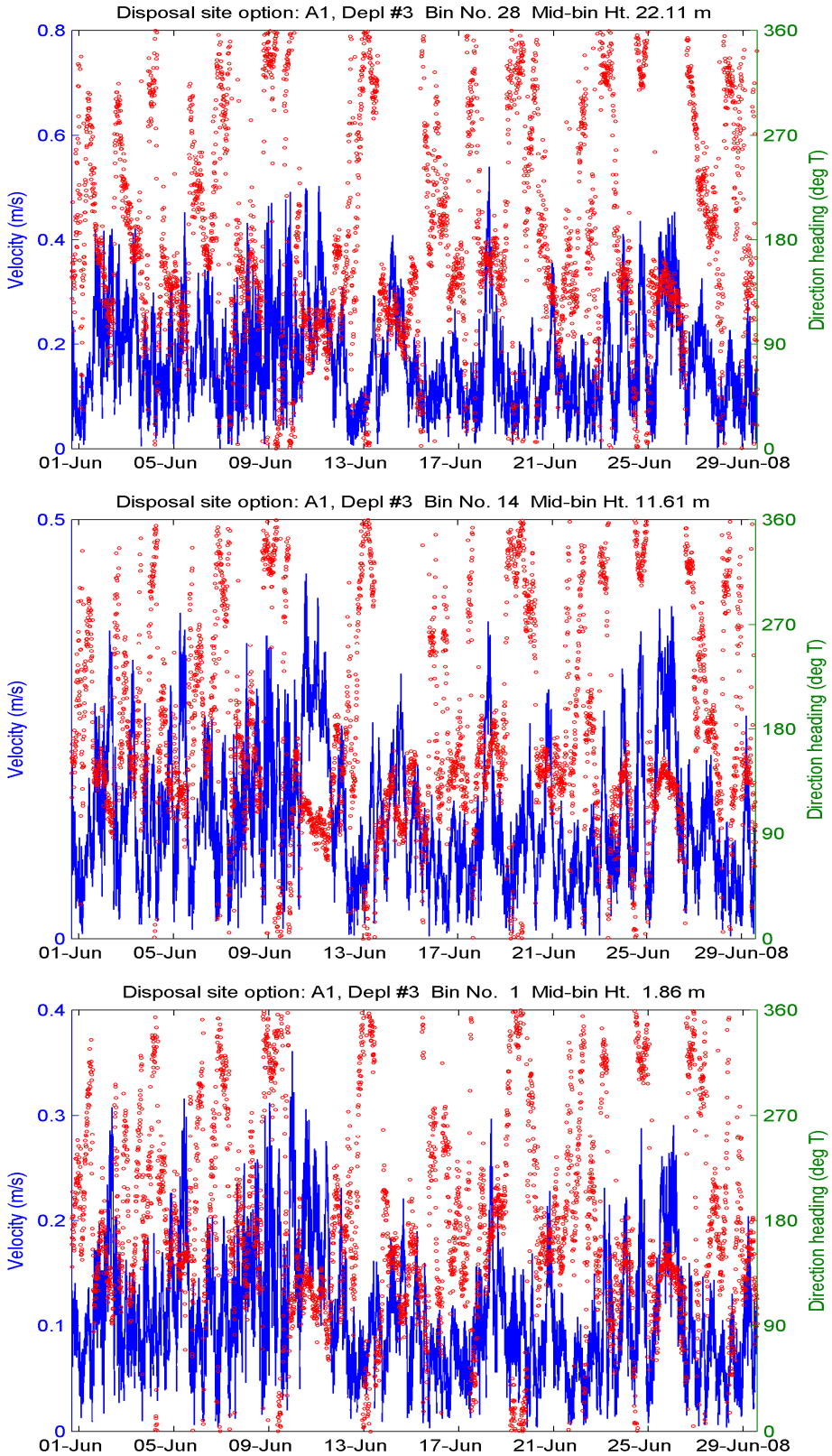

Figure 5.23: Current speeds (blue lines, left-hand scale) and directions (red dots, right-hand scale) at 3 different elevations above the bed for deployment A1 /3.

Figure 5.24 shows the time series of water depth above the ADCP sensor (add 0.4 m for total water depth) and the near-bed sea temperature for deployment A1 /3. Water temperature near the seabed oscillated mainly between 10–11°C, with rapid rises and falls of around 0.7°C occurring during stronger wind events.

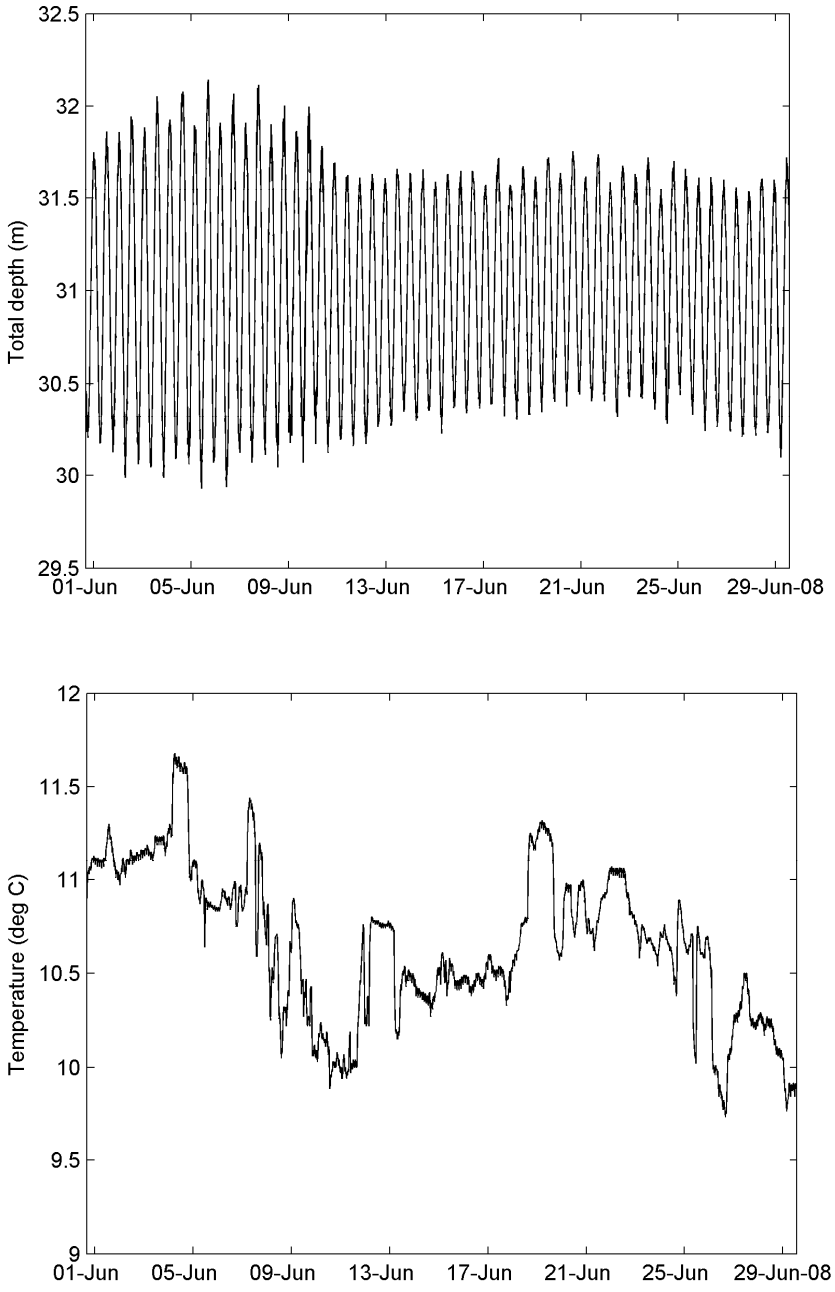

Figure 5.24: Water depth (TOP) and near-bed sea temperature (BOTTOM) for deployment A1 /3.

Winds that span the deployment period are shown in Figure 5.25, with the strongest wind speed of 28 m/s occurring on 8 June during a sustained WSW wind period.

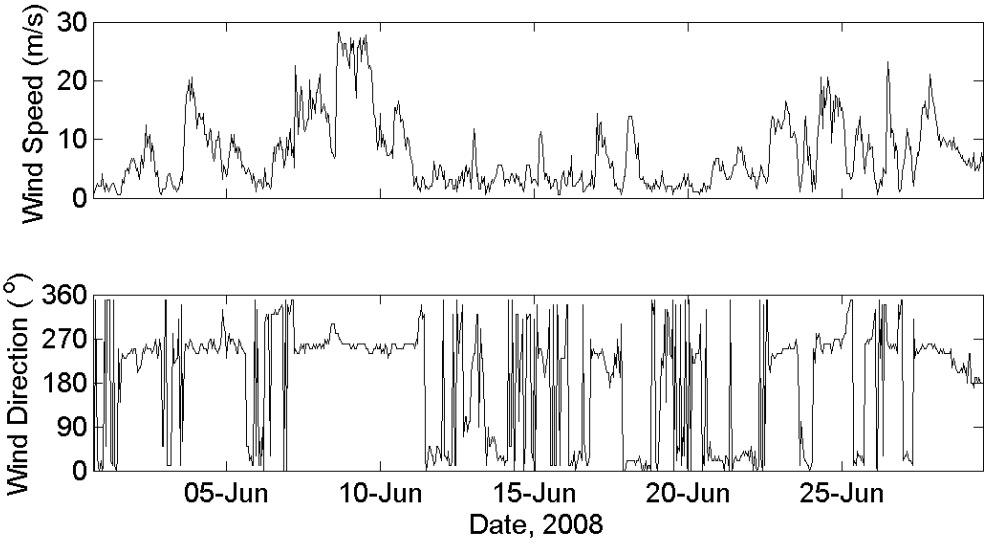

Figure 5.25: Wind speed (m/s) and direction (in meteorological convention "blowing from") at Taiaroa Head for deployment 3.

The scatter plots of all velocities measured for two vertical bins (near seabed and upper water column) are shown in Figure 5.26 with the resulting principal component analysis in Table 5.9.

At both depths (Figure 5.26), the currents are distributed reasonably evenly in different directions, but the larger currents have a preferred orientation (major axis) in the same SE direction as demonstrated in both deployments 1 and 2. The principal (major) current directions and standard deviations listed in Table 5.9 are quite similar and consistent with the results from deployments 1 and 2 (Tables 5.5 & 5.7), although the standard deviation of the currents was higher in deployment 3.

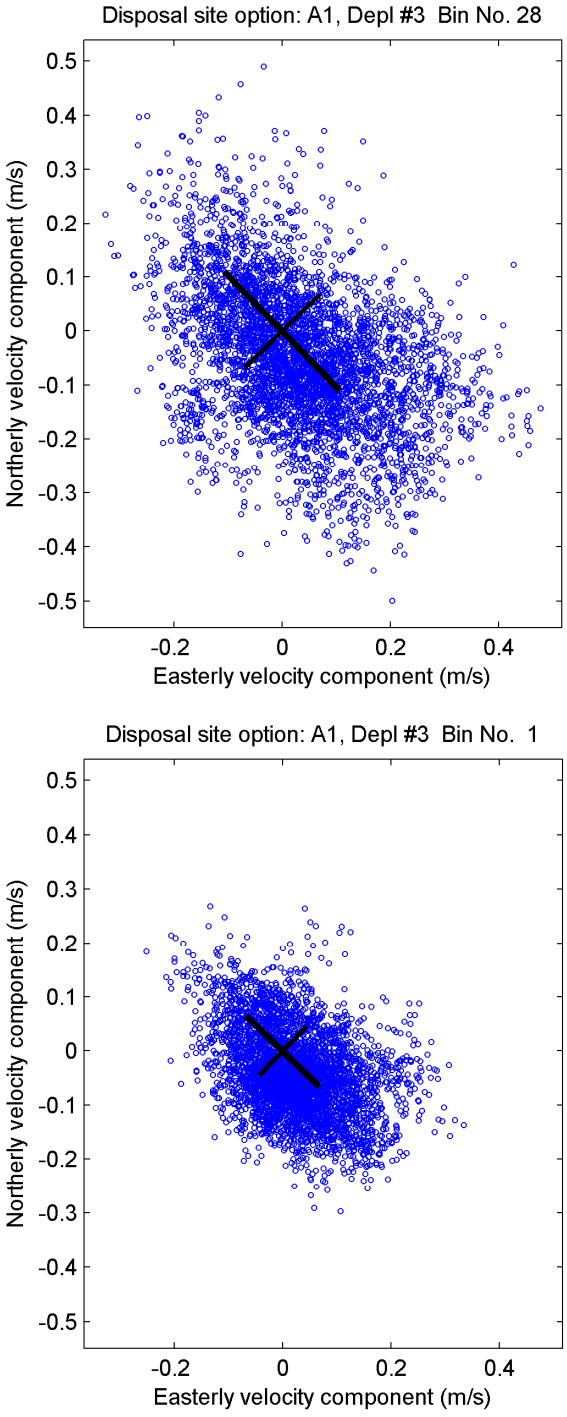

Figure 5.26: Scatter plots for currents at two bin heights from deployment A1 /3, based on the east-west current component (x-axis) and the north-south current component (y-axis). The thick line is the major principal axis, where the standard deviation is a maximum and the thinner line is the minor principal axis—both lines span ± 1 standard deviations in m/s.

Table 5.9: Summary of principal component analysis for currents during deployment A1 /3.

Bin No./depth	Major axis orientation (°True North)	Major axis std. dev (m/s)	Minor axis std. dev. (m/s)
28 (22.1 m)	136°	±0.152	±0.097
14 (11.6 m)	130°	±0.129	±0.075
1 (1.9 m)	134°	±0.093	±0.062

Figure 5.27 shows the progressive-vector plots for deployment A1 /3 at three bin heights in the water column. At all depths, the current drift was again consistently towards the SE, with some minor meanders between 7–10 June (during the strong WSW event; Figure 5.23) and 19–23 June (NE winds switching to WSW). There was also a deviation to a more easterly orientation in the drift direction between 10–15 June, probably caused by the relaxation from a strong WSW event to a calmer period (Figure 5.25). The net current drift velocities and directions are listed in Table 5.10. The net drift velocities were somewhat higher than during the previous deployment (Table 5.8), and the net drift direction swung round slightly more to the east to be closer to a SE direction.

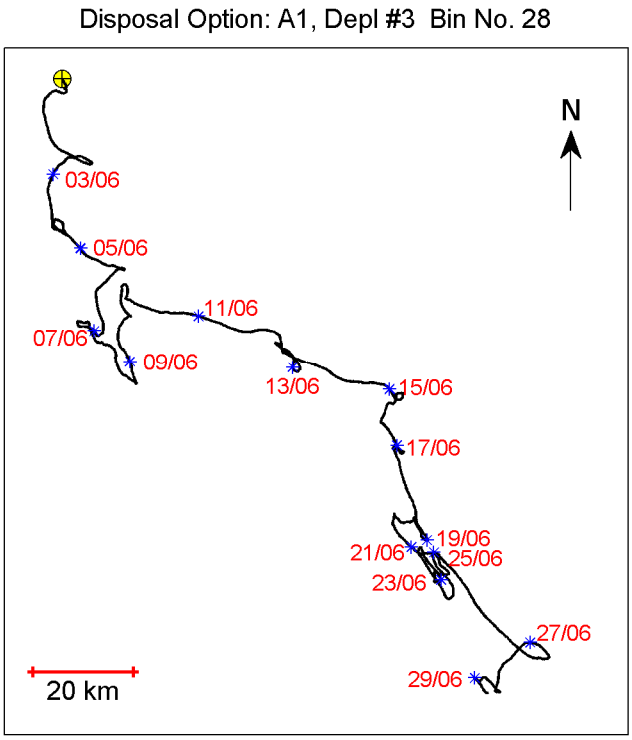

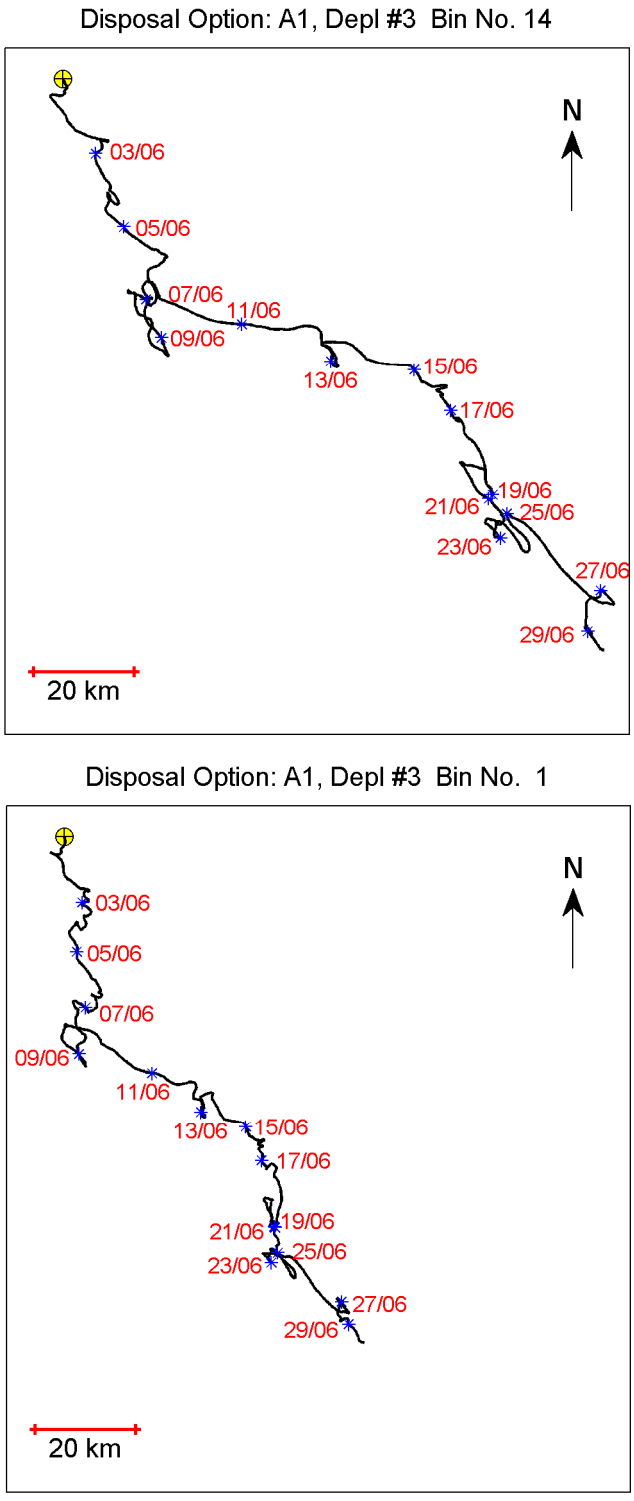

Figure 5.27: Progressive current drift at 3 depths from ADCP deployment A1 /3 starting 1620 31-May (yellow cross) through to 1400 29-Jun-2008 (28.91 days). Every second day (0000 hrs) is marked by an asterisk and date-stamped in day/month format.

Table 5.10: Summary of the overall current drift during deployment A1 /3 (28.9 days).

Bin No./depth	Net drift velocity (m/s)	Net drift velocity (km/day)	Mean drift direction (°True North)
28 (22.1 m)	0.060	5.14	145°
14 (11.6 m)	0.063	5.41	137°
1 (1.9 m)	0.047	4.05	149°

Wave statistics were also extracted from the 20-minute bursts every 2 hours during deployment A1 /3 and are shown in Figure 5.28. Wave direction is expressed in the same convention as winds—the direction from which waves arrive from.

The highest significant wave height of 2.9 m was reached at 2200 h on 08 June 2008, with peak spectral periods of 12–14 seconds (swell) arriving from a SSE direction. The local winds at Taiaroa Head preceding this peak were strong west to WSW winds.

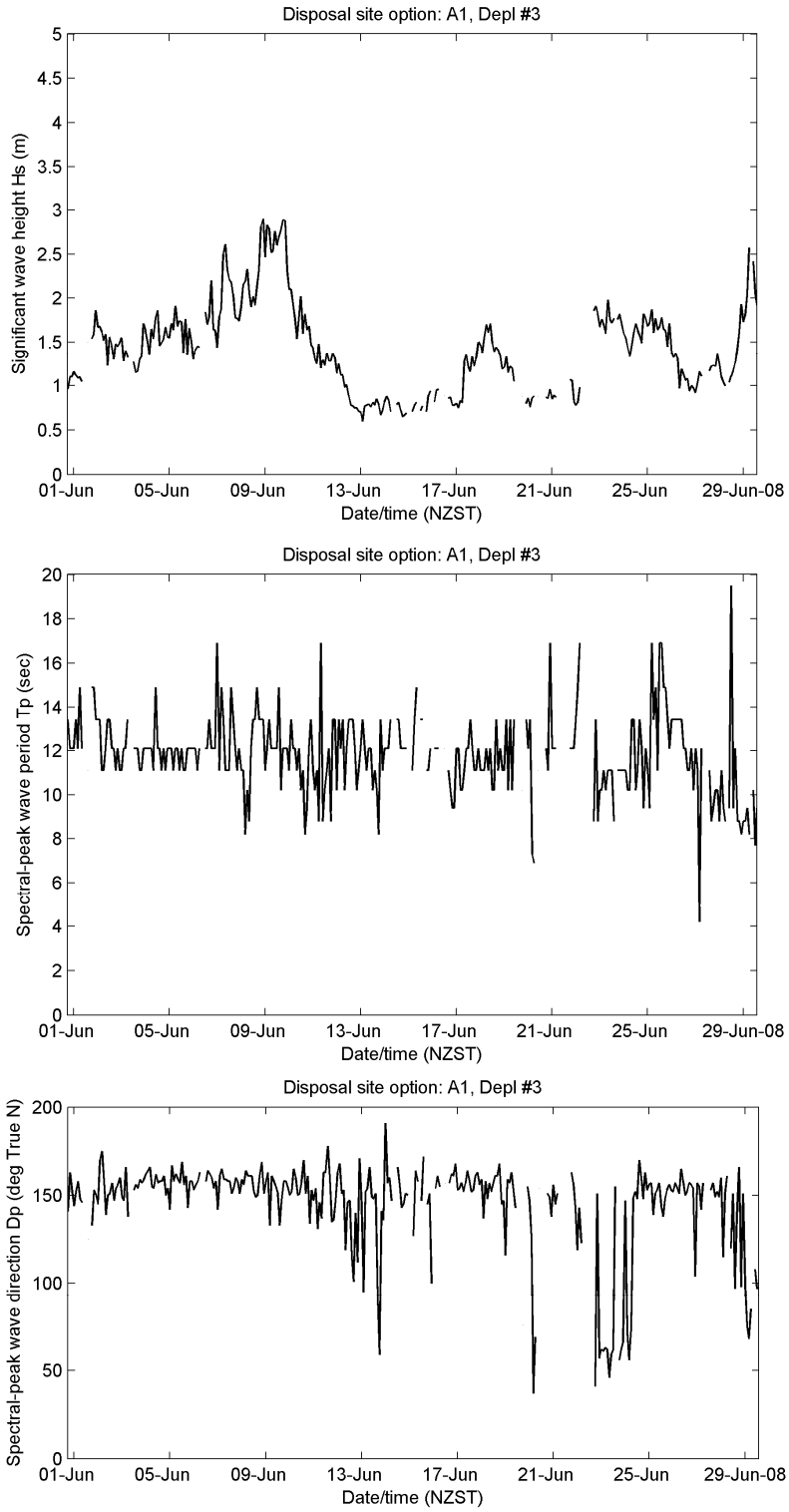

Figure 5.28: Wave statistics from deployment A1 /3: (top) significant wave height (H_s); (middle) spectral peak period (T_p); (bottom) spectral peak wave direction (D_p).

5.2.4 Deployment A1 /4

The set of time series plots for currents from deployment A1 /4 from 04 July to 04 Aug are shown in Figure 5.29 for three vertical elevations above the seabed (Bin #1 at 1.9 m, Bin #14 at 11.6 m and Bin #28 at 22.1 m).

The highest current speed near the seabed (Bin #1) reached 0.44 m/s at 1400 hours on 5 July, following a period of strong WSW winds up to 25 m/s. This was the highest current speed measured in Bin #1 throughout all four deployments. The maximum current in Bin #14 of 0.60 m/s also occurred at the same time. In the upper bin (Bin #28), the maximum current was measured on 25 July at 0.81 m/s, after a 40-hour period of winds from the south that locally peaked at 10–14 m/s, but offshore southerly winds may have had a greater influence on shelf currents.

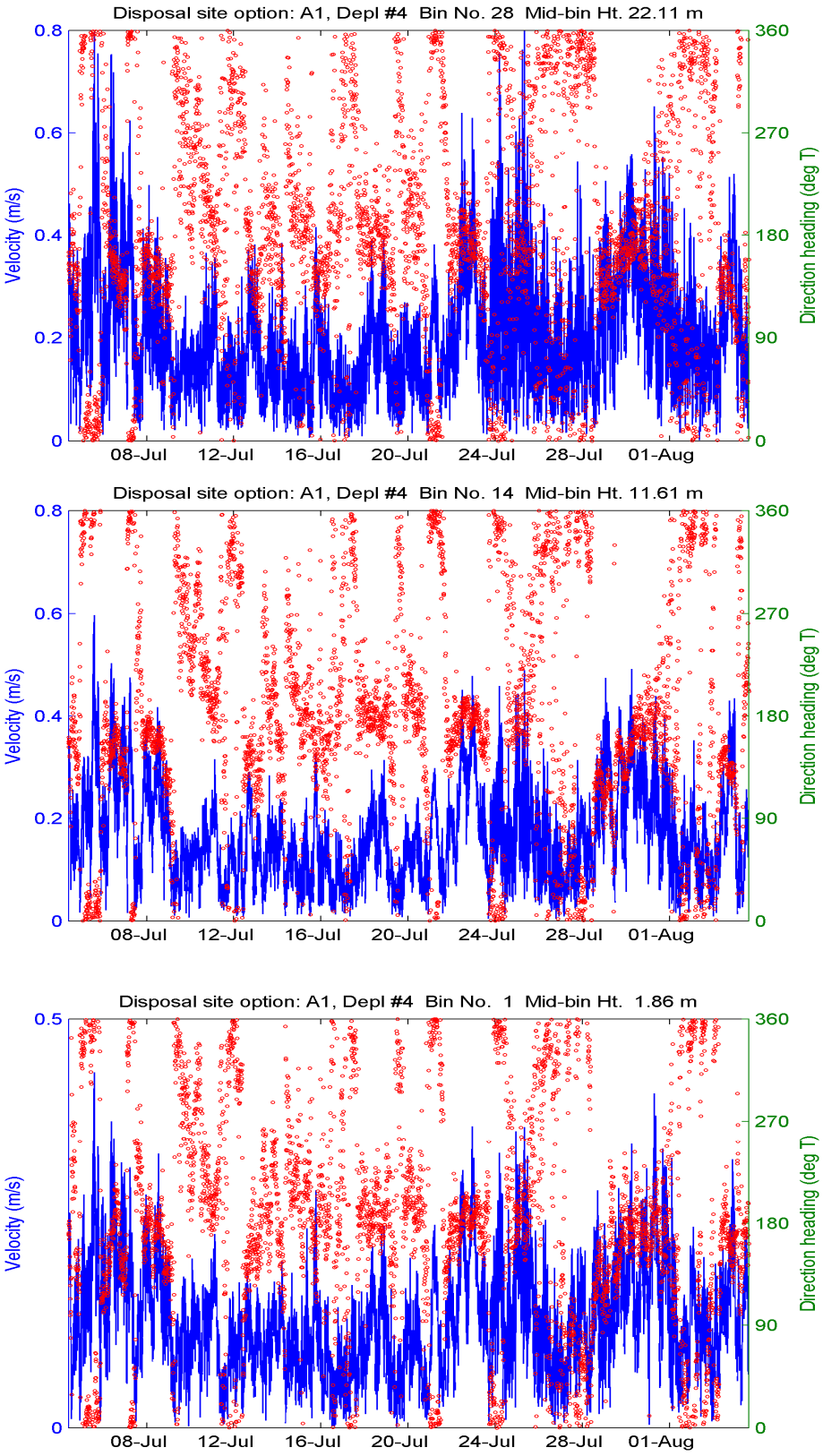

Figure 5.29: Current speeds (blue lines, left-hand scale) and directions (red dots, right-hand scale) at 3 different elevations above the bed for deployment A1 /4.

Figure 5.30 shows the time series of water depth above the ADCP sensor (add 0.4 m for total water depth) and the near-bed sea temperature for deployment A1 /4. Water temperature near the seabed oscillated substantially between 9–10.5°C, followed by a steady decline from 24 July with the onset of the southerly wind event.

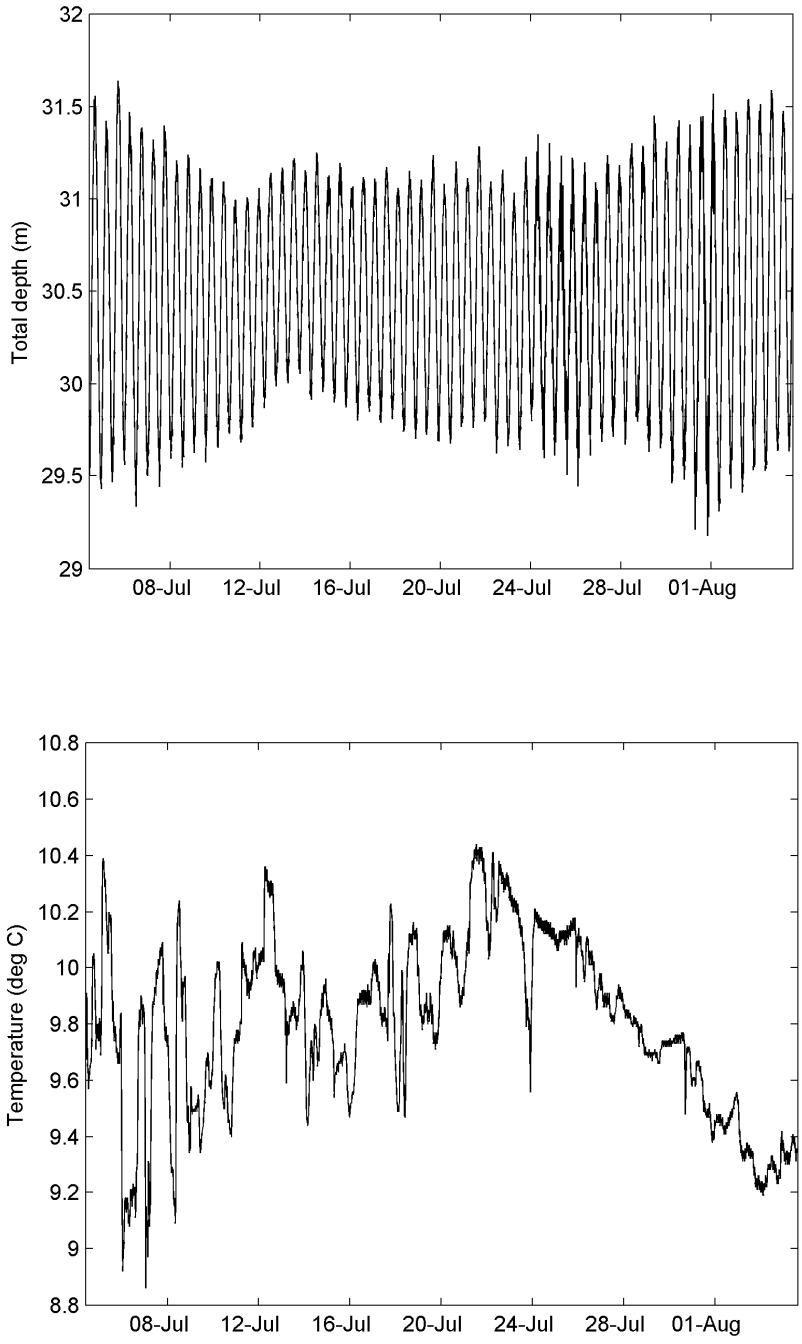

Figure 5.30: Water depth (TOP) and near-bed sea temperature (BOTTOM) for deployment A1 /4.

Winds that span the deployment period are shown in Figure 5.31, with the strongest wind speed of 25 m/s occurring on 5 July during a WSW wind period.

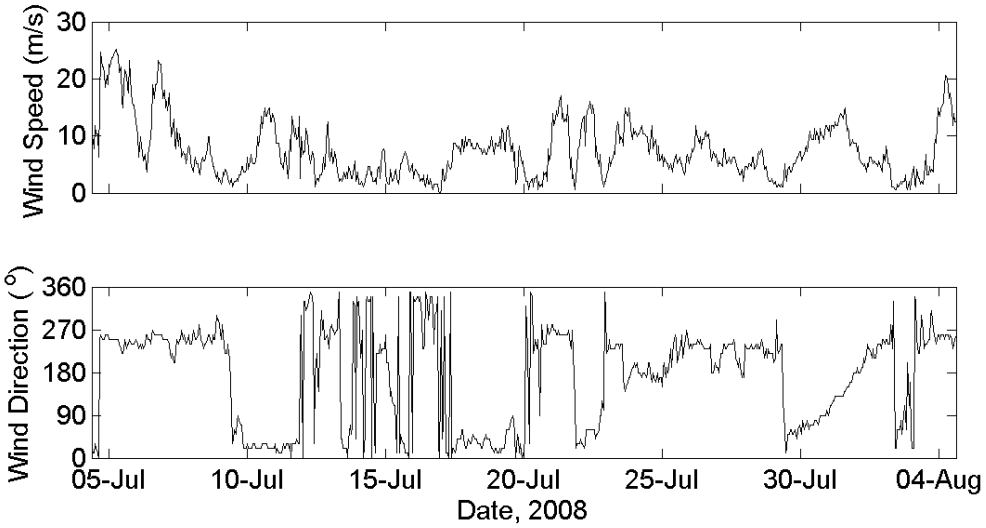

Figure 5.31: Wind speed (m/s) and direction (in meteorological convention "blowing from") at Taiaroa Head for deployment 4.

The scatter plots of all velocities measured for two vertical bins (near seabed and upper water column) are shown in Figure 5.32 with the resulting principal component analysis in Table 5.11.

At both depths (Figure 5.32), the currents are distributed reasonably evenly in different directions, but the larger currents have a preferred orientation (major axis) in a SSE direction in Bin #28 and more to the south near the seabed (Bin #1), which is a slight change to the very consistent direction for the maximum current speeds demonstrated in deployments 1 to 3. The principal (major) current directions and standard deviations listed in Table 5.11 reveal a deviation from the fairly consistent pattern shown previously for the major-axis orientation, which swung round more to a north-south orientation, with a higher standard deviation for the currents in all vertical bins than in the previous deployments.

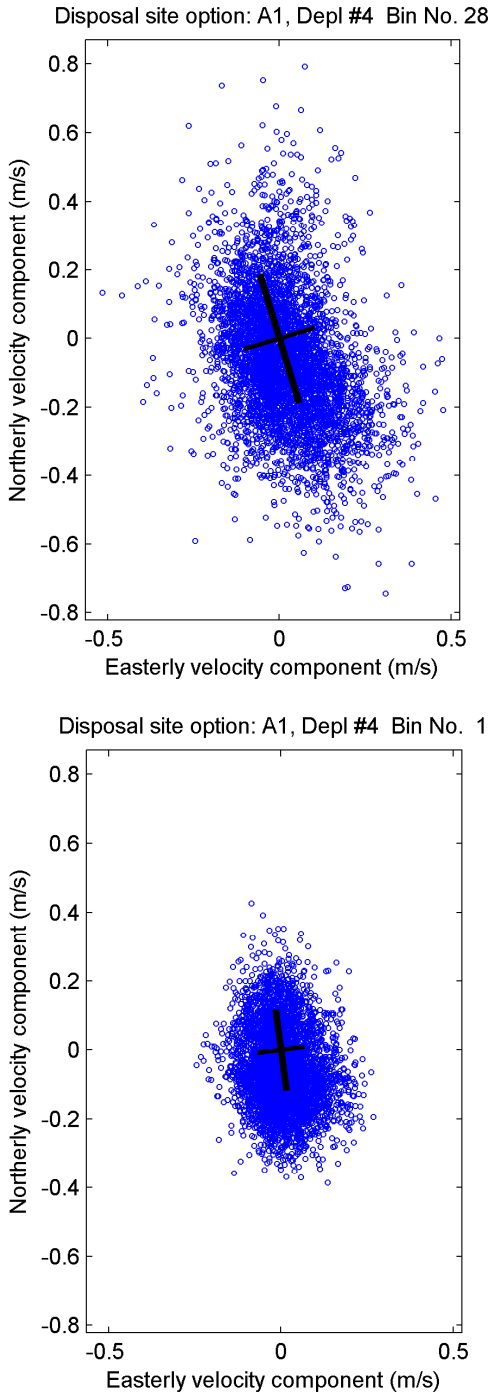

Figure 5.32: Scatter plots for currents at two bin heights from deployment A1 /4, based on the east-west current component (x-axis) and the north-south current component (y-axis). The thick line is the major principal axis, where the standard deviation is a maximum and the thinner line is the minor principal axis—both lines span ± 1 standard deviations in m/s.

Table 5.11: Summary of principal component analysis for currents during deployment A1 /4.

Bin No./depth	Major axis orientation (°True North)	Major axis std. dev (m/s)	Minor axis std. dev. (m/s)
28 (22.1 m)	163°	±0.194	±0.106
14 (11.6 m)	163°	±0.157	±0.084
1 (1.9 m)	172°	±0.118	±0.068

Unlike the scatter plots, progressive-vector or drift plots show the time sequence of currents as shown in Figure 5.33 for deployment A1 /4 at three bin heights in the water column. At all depths, the current drift was consistent, but more towards the south compared with the previous three deployments. The deviation to a more southerly drift was most noticeable in the period from 10–20 July (see Bin #1 plot in Figure 5.33), which coincided with strong NNE winds interspersed with calmer SW breezes (Figure 5.31). There were occurrences of a reversal in the net drift, particularly on 23-24 July and 31 July to 1 August, which coincided with periods of SE to south winds, with the drift to the south recommencing with the onset of winds from the SW quarter. This change in pattern of the net current drift shows the importance of the sequencing of winds from the SE quarter or extended periods of stronger NNE winds interspersed with calmer periods, even if winds are light from the SW quarter. Otherwise the prevailing current drift in most cases is to the SE as measured in the previous three deployments. This result has implications for the hydrodynamic and sediment modelling for a disposal ground offshore (Bell et al. 2009), with tides being negligible, the Southland Current providing the regional context for mean flows, and the winds being the predominant cause of variability of current drift in the area of A1.

The net current drift velocities and directions are listed in Table 5.12. The net drift velocities were similar to deployment 3 (Table 5.10), but the mean drift directions swung round more to the west to be closer to a southerly direction near the seabed.

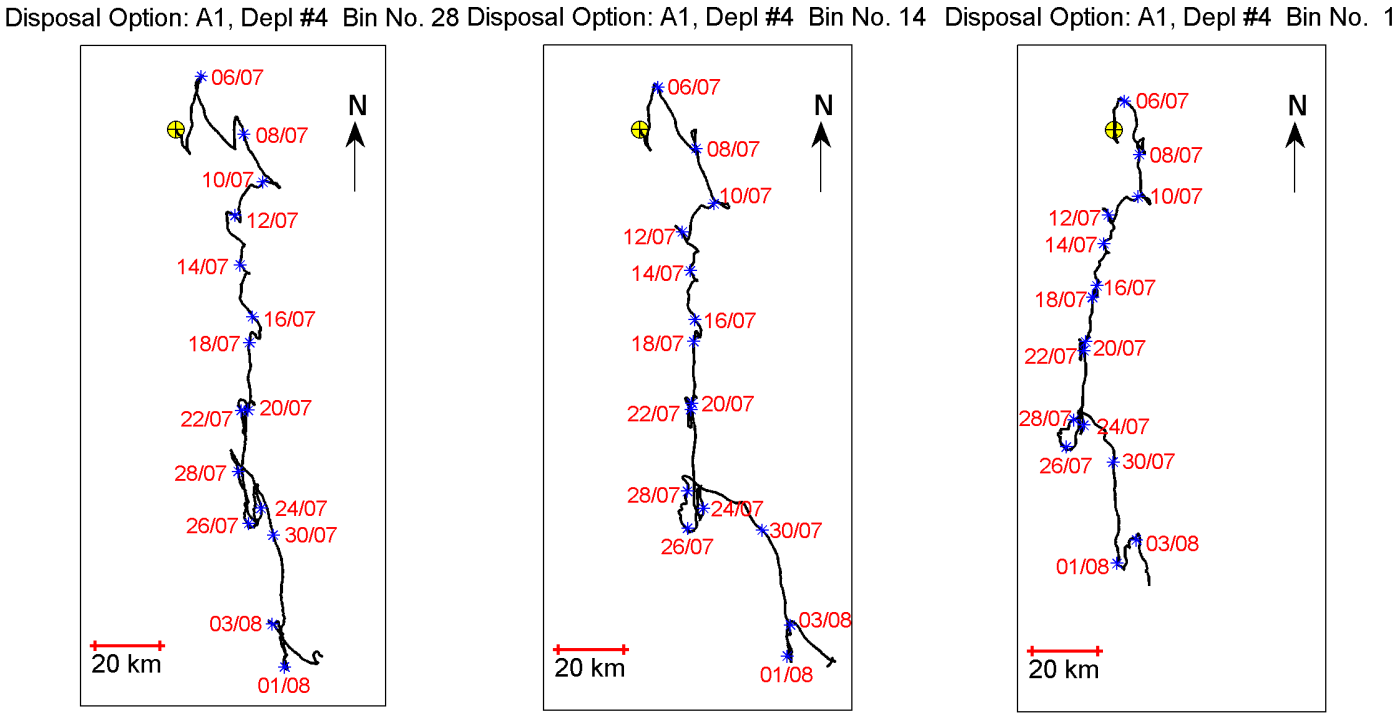

Figure 5.33: Progressive current drift at 3 depths from ADCP deployment A1 /4 starting 0950 4-Jul (yellow cross) through to 1500 8-Jul-2008 (31.21 days). Every second day (0000 hrs) is marked by an asterisk and date-stamped in day/month format.

Table 5.12: Summary of the overall current drift during deployment A1 /4 (31.2 days).

Bin No./depth	Net drift velocity (m/s)	Net drift velocity (km/day)	Mean drift direction (°True North)
28 (22.1 m)	0.063	5.41	164°
14 (11.6 m)	0.065	5.58	161°
1 (1.9 m)	0.052	4.48	177°

Wave statistics were also extracted from the 20-minute bursts every 2 hours during deployment A1 /4 and are shown in Figure 5.34. Wave direction is expressed in the same convention as winds—the direction from which waves arrive from.

The three largest wave events of the entire field period were measured during this 4th deployment. The highest significant wave height of 4.7 m was reached at 1800 h on 31 July 2008, with peak spectral periods of 11–13 seconds (swell) arriving from an easterly direction. The local winds at Taiaroa Head preceding this peak were from the

SE. The second highest significant wave height of 4.5 m was reached a week earlier at 0600 h on 24 July 2008, with peak spectral periods of 10–12 seconds (swell) arriving from a SE direction, with local winds blowing from the south. The third highest significant wave height of 3.1 m was measured near the start of the deployment at 0800 h on 5 July, with 10-12 second peak spectral periods and arriving from SSE.

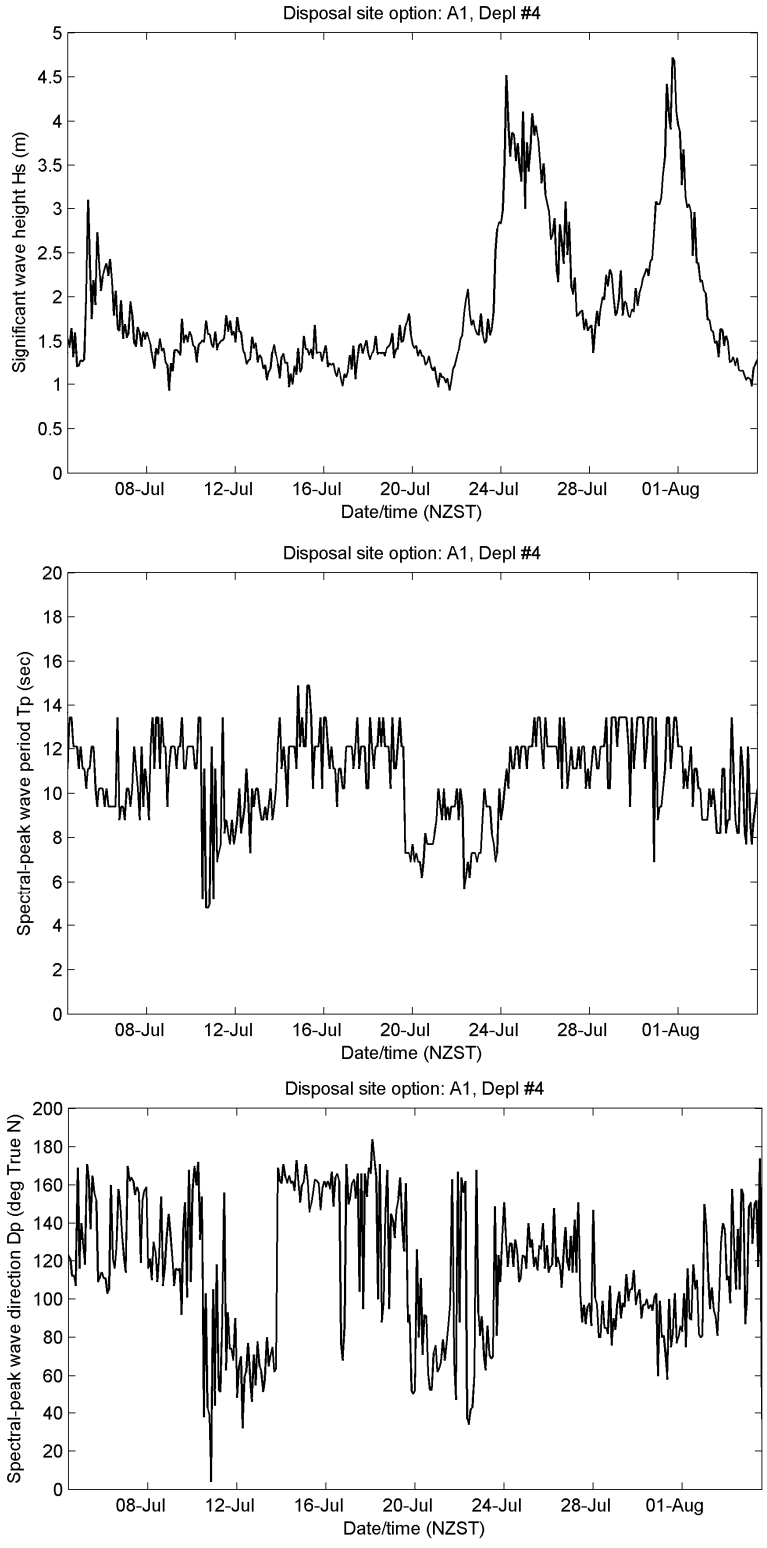

Figure 5.34: Wave statistics from deployment A1 /4: (top) significant wave height (H_s); (middle) spectral peak period (T_p); (bottom) spectral peak wave direction (D_p).

5.3 Heyward Point (Site B2)

One ADCP deployment was carried out at site B2 after the ADCP mooring was moved from B1 to obtain current velocity and wave data inshore near the existing disposal grounds used for maintenance dredging. Details of the location and periods listed in Tables 2.1 to 2.2. There was a malfunction of the ADCP for several hours on 15 July before recording started again resulting in a short gap in the middle of the data record.

5.3.1 Deployment B2 /1

The set of time series plots for currents from deployment B2 /1 from 04 July to 04 August are shown in Figure 5.35 for 3 vertical elevations above the seabed (Bin #1 at 1.9 m, Bin #10 at 8.6 m and Bin #15 at 12.4 m).

A high current speed occurred at 1830 h on 31 July, reaching 1.0 m/s near the seabed (Bin #1) and 1.1 m/s in Bin #15. These high currents inshore off Heyward Point were caused by a period of initially easterly winds that turned to SE winds, with wind speeds up to 15 m/s locally (Taiaroa Head). This alongshore-orientated SE wind generated these high currents downwind parallel to the coast towards Blueskin Bay in a direction 293° True North at all depth levels. However, most of the time the currents near the seabed (Bin #1) were less than 0.3 m/s, apart from two brief episodes on 24 and 25 July (Figure 5.35) with currents peaking at 0.5 and 0.59 m/s, respectively, during southerly winds.

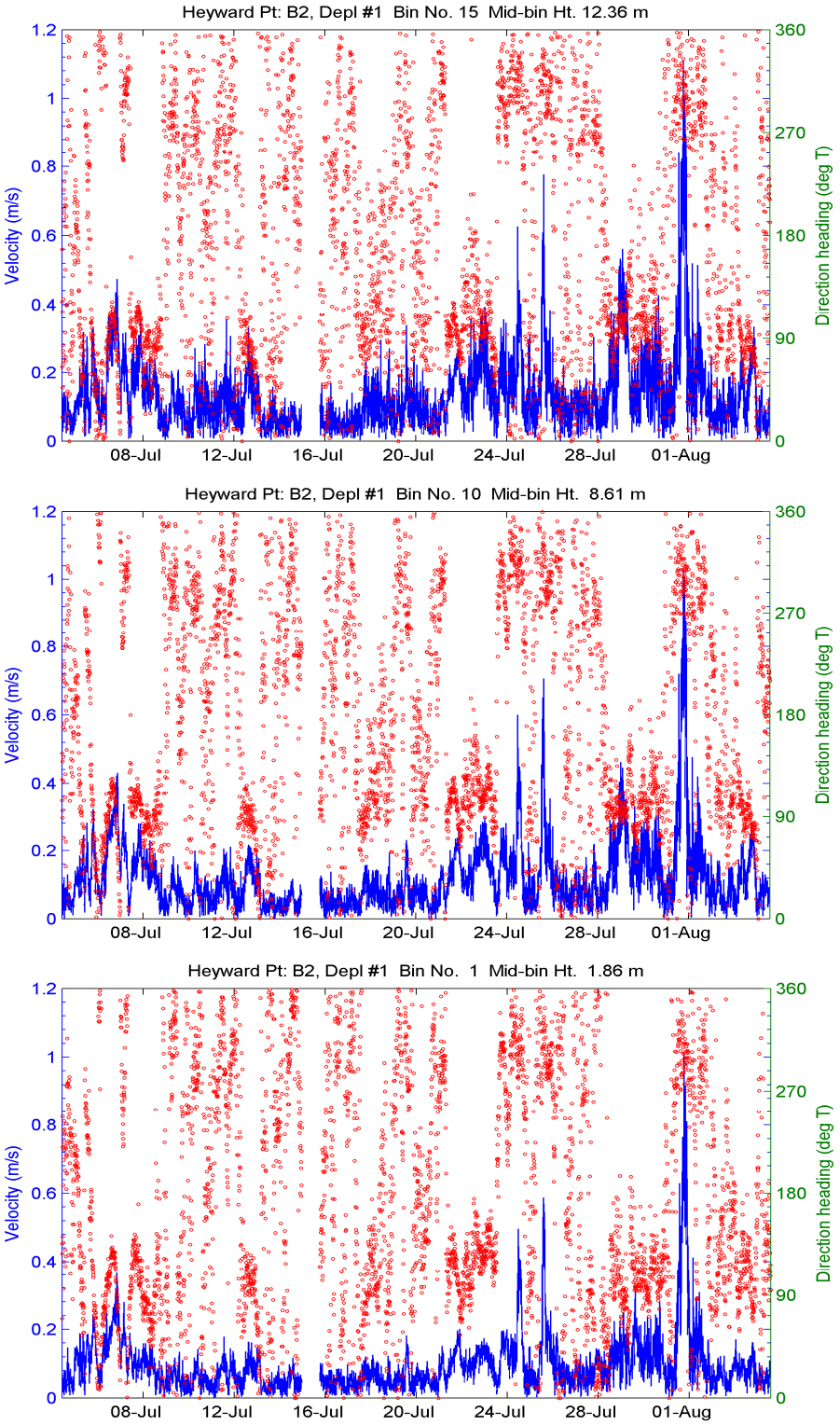

Figure 5.35: Current speeds (blue lines, left-hand scale) and directions (red dots, right-hand scale) at 3 different elevations above the bed for deployment B2 /1.

Figure 5.36 shows the time series of water depth above the ADCP sensor (add 0.4 m for total water depth) and the near-bed sea temperature for deployment B2 /1. Water temperature near the seabed oscillated up and down in a similar manner to the concurrent offshore mooring site at A1 (Figure 5.30) with a similar steady decline from the 24 July with the onset of the south to SE wind episode. As expected in winter, sea temperatures were cooler inshore—in this case B2 was approximately 0.2°C cooler than the deeper offshore A1 deployment.

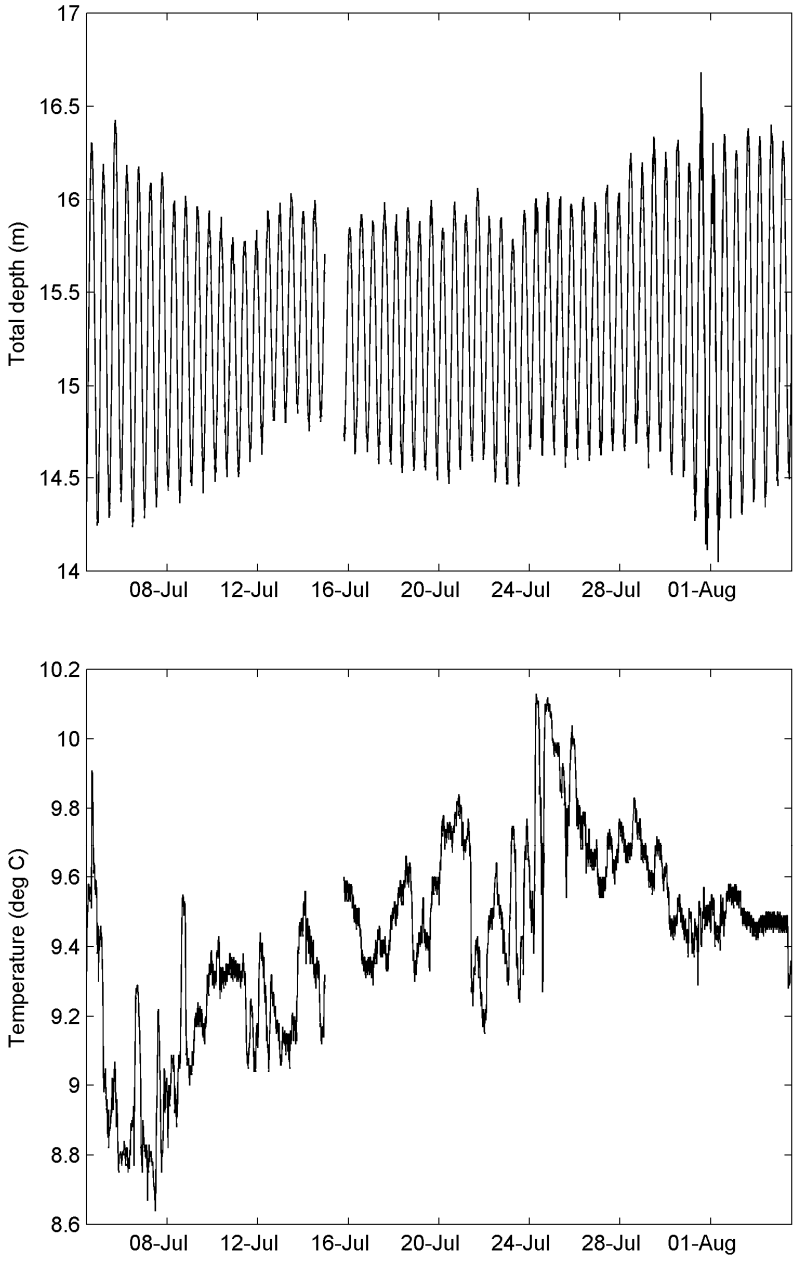

Figure 5.36: Water depth (TOP) and near-bed sea temperature (BOTTOM) for deployment B2 /1.

Winds that span the deployment period are shown in Figure 5.37, with the strongest wind speed of 25 m/s occurring on 5 July during a WSW wind period.

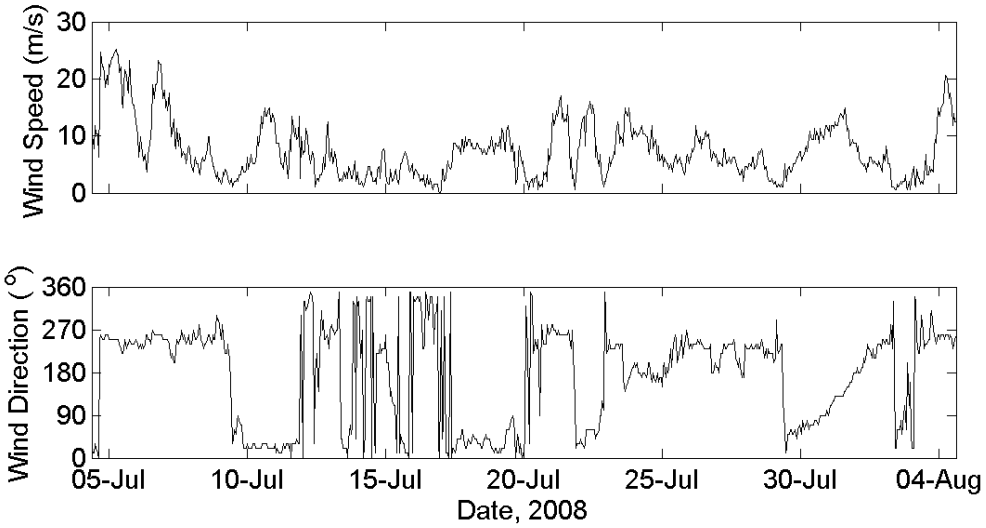

Figure 5.37: Wind speed (m/s) and direction (in meteorological convention "blowing from") at Taiaroa Head for deployment B2 /1.

Based on a tidal analysis of currents near the seabed (Bin #1) over the 1-month record, the tidal currents that could be resolved only explain a small 5% of the variability in the current velocities off Heyward Point. Normally this percentage would be somewhat higher, but for this deployment the current variability was dominated by the SE wind event of 31 July. The main twice-daily lunar tide (M_2) is quite small, peaking at 0.025 m/s (compared to an even smaller 0.015 m/s at B1 in Blueskin Bay) along an axis oriented ENE–WSW (57–237° True North). In Bin #15 (12.4 m above seabed), the peak M_2 tidal current was higher at 0.033 m/s, with tides explaining only 3% of the total variability. So wind is the dominant forcing for currents off Heyward Point, even though it is close to Otago Harbour entrance.

The scatter plots of all velocities measured for two vertical bins (near seabed and upper water column) are shown in Figure 5.38 along with the resulting principal component analysis. Each velocity is plotted according to its east-west (horizontal axis) and north-south (vertical axis) components of speed (m/s). The major principal axis (thick line in Figure 5.38) is the orientation where the standard deviation or variability of the currents is a maximum, and its length is ±1 standard deviation (Table 5.13). The perpendicular minor principal axis is marked by the thin line based on the standard deviation listed in Table 5.13.

At both depths (Figure 5.38), the currents are mostly distributed in an elliptical pattern in a preferred orientation of SE/NW but the larger velocities in the NW direction were recorded during the SE and S wind episodes. The principal (major) current directions and standard deviations listed in Table 5.13 reveal a consistent pattern with depth, with decreasing standard deviation in current speeds approaching the seabed.

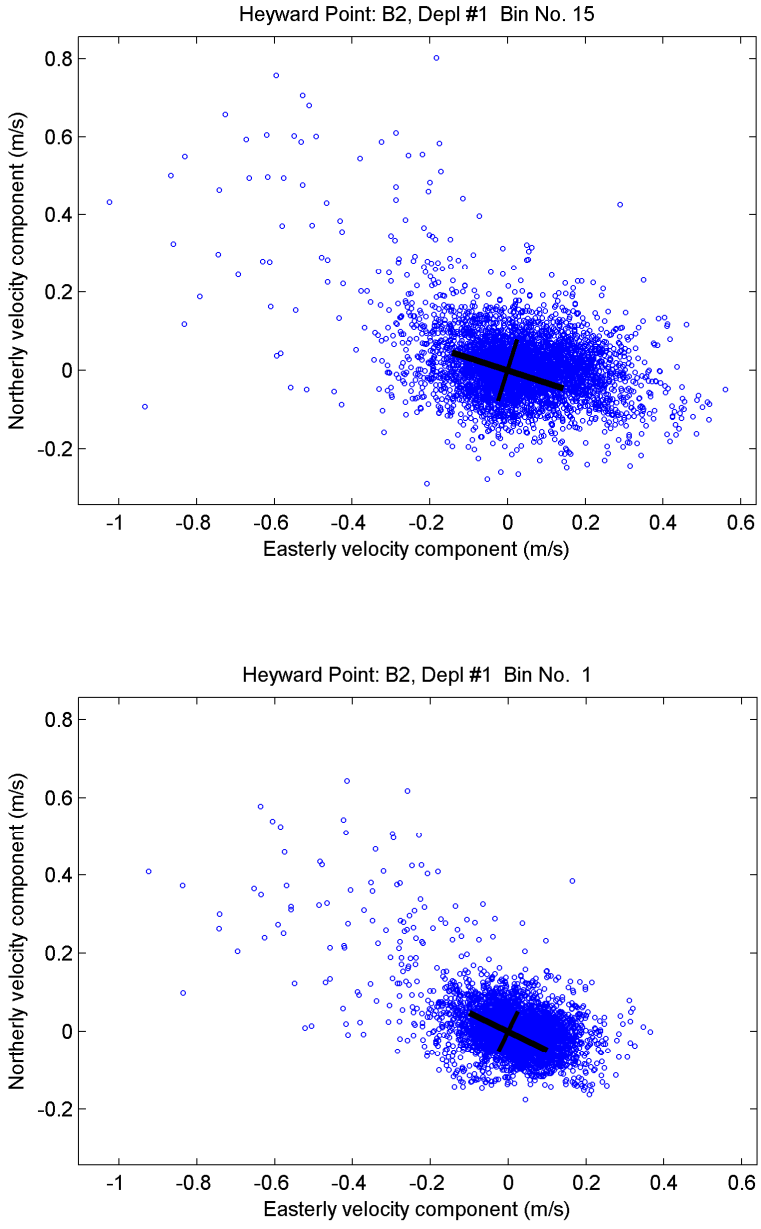

Figure 5.38: Scatter plots for currents at two bin heights from deployment B2 /1, based on the east-west current component (x-axis) and the north-south current component (y-axis). The thick line is the major principal axis, where the standard deviation is a maximum and thinner line is minor principal axis—both lines span ± 1 standard deviations in m/s.

Table 5.13: Summary of principal component analysis for currents during deployment A1 /4.

Bin No./depth	Major axis orientation (°True North)	Major axis std. dev (m/s)	Minor axis std. dev. (m/s)
15 (12.4 m)	108°	±0.15	±0.082
10 (8.6 m)	109°	±0.14	±0.067
1 (1.9 m)	116°	±0.11	±0.056

Figures 5.39a-b show the progressive-vector plots for deployment B2 /1 at three bin heights in the water column. The drift plots are plotted separately for the first and second part of the deployment due to a break of nearly 1 day in the record arising from an ADCP malfunction. For the first part of the deployment (Figure 5.39a) covering 10.5 days (4–14 July), the drift pattern to the east towards the outer approach channel was quite similar throughout the water column, with the expected lower drift velocity near the seabed. The greatest current drift occurred on 5–7 July during an extended SW wind episode with wind speeds up to 25 m/s moving the water over site B2 to the east.

For the second part of the deployment (Figure 5.39b) covering a longer 19.8 days (15 July to 4 August), the drift pattern was to the NE in a series of four to-and-fro movements in an ESE then NW direction. This pattern can be explained by the winds. The east to ESE drift occurred during either SW or NE winds, which along with Figure 5.39a suggests this is the prevailing current drift direction at B2. The switch to the alternate current drift direction to the NW (late 23 to 27 July and 31 July to 1 Aug) coincided with a switch to winds from the south to SE direction.

The net current drift velocities and directions for the combined drift plots in Figure 5.39a and b are listed in Table 5.14. The net drift velocity near the seabed was approximately 1 km/day, and the prevailing current-drift direction was to the ENE.

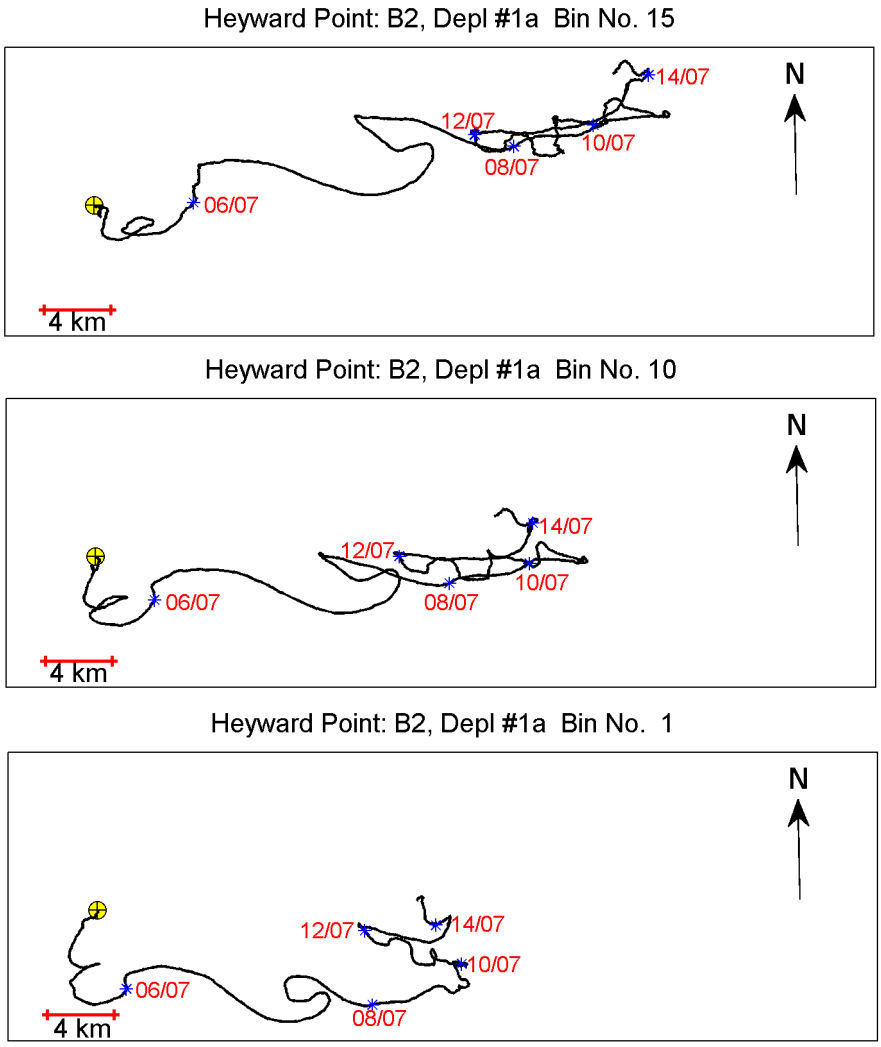

Figure 5.39a: Progressive current drift at 3 depths from the 1st part of ADCP deployment B2 /1 starting 1020 4-July (yellow cross) through to 2310 14-Jul-2008 (10.53 days). Every second day (0000 hrs) is marked by an asterisk and date-stamped in day/month format.

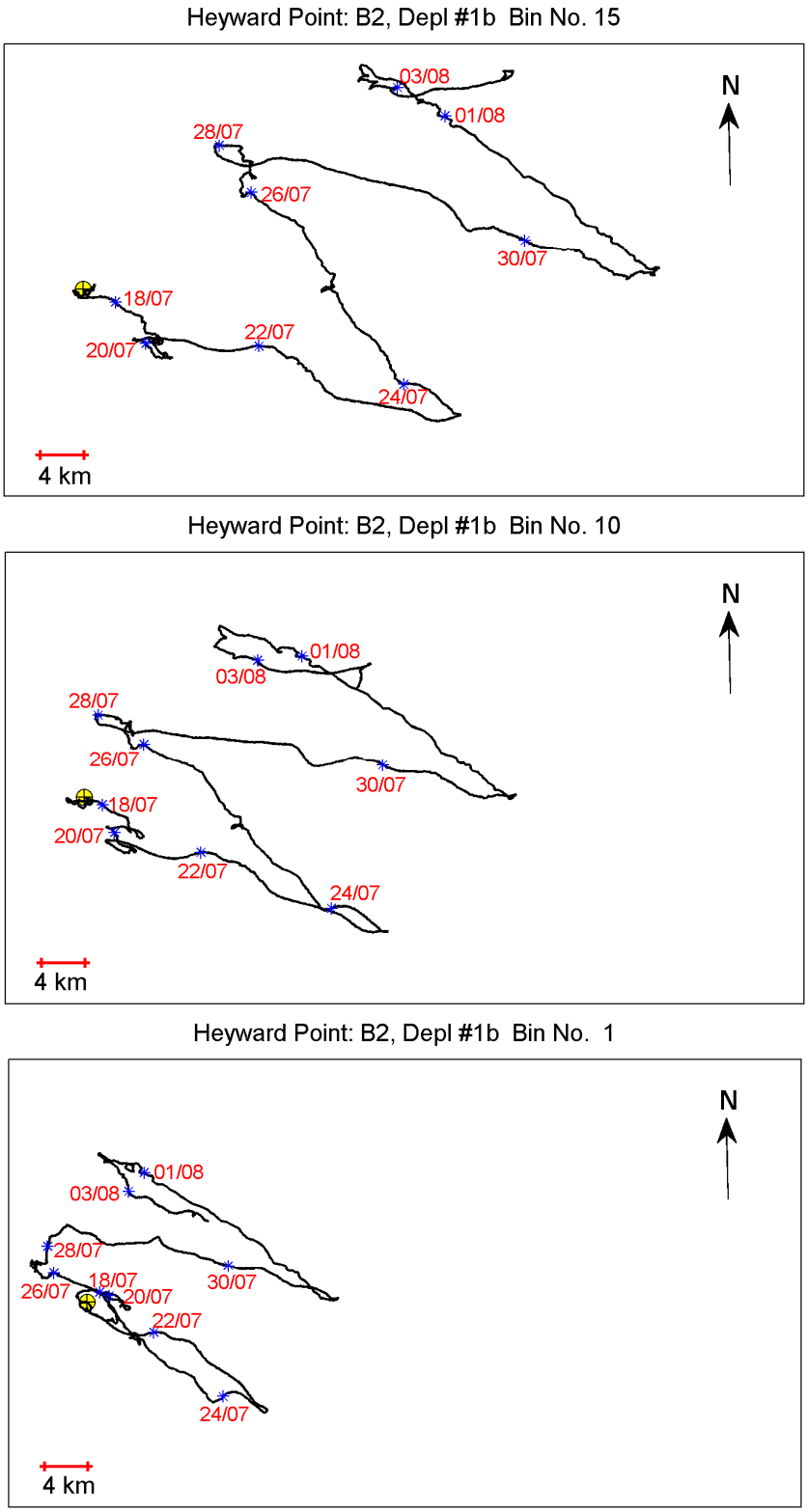

Figure 5.39b: Progressive current drift at 3 depths from the 2nd part of ADCP deployment B2 /1 starting 1900 15-July (yellow cross) through to 1350 4-Aug-2008 (19.82 days). Every second day (0000 hrs) is marked by an asterisk and date-stamped in day/month format.

Table 5.14: Summary of the overall current drift during deployment B2 /1, which combines the weighted drift excursions from Figures 5.35a and 5.35b (total of 30.36 days) and excludes the gap of nearly 1-day in the middle of the deployment arising from an ADCP malfunction.

Bin No./depth	Net drift velocity (m/s)	Net drift velocity (km/day)	Mean drift direction (°True North)
28 (22.1 m)	0.029	2.48	69°
14 (11.6 m)	0.019	1.68	76°
1 (1.9 m)	0.012	1.05	75°

Wave statistics were also extracted from the 20-minute bursts every 2 hours during deployment B2 /1 and are shown in Figure 5.40 along with the wave statistics from the concurrent deployment at A1 (also plotted separately in Figure 5.34). Wave direction is expressed in the same convention as winds—the direction from which waves arrive from.

The main features arising from this comparison are:

- The significant wave height is substantially lower further inshore at site B2 as expected, due mainly to sheltering by the Otago Heads. However, the highest wave event on 31 July with waves arriving directly onshore from the east shows the reduction in peak wave height was only 16% (4.0 m at B2 compared to 4.7 m at A1). In contrast, the waves were substantially dampened at site B2 during the other large wave event on 24 July because of sheltering by the Heads.

- The peak spectral periods were similar for most of the deployment, except during some occasions when a mixed sea was present, when the wave period dropped at B2 as the swell was reduced by the sheltering effect of the Heads.

- At B2, the spectral peak wave direction was in a much narrower band of 60–100° true North, compared to the open offshore site at A1. This feature arises from the refraction of waves from both the south and north into a more onshore-directed wave train closer to the coast.

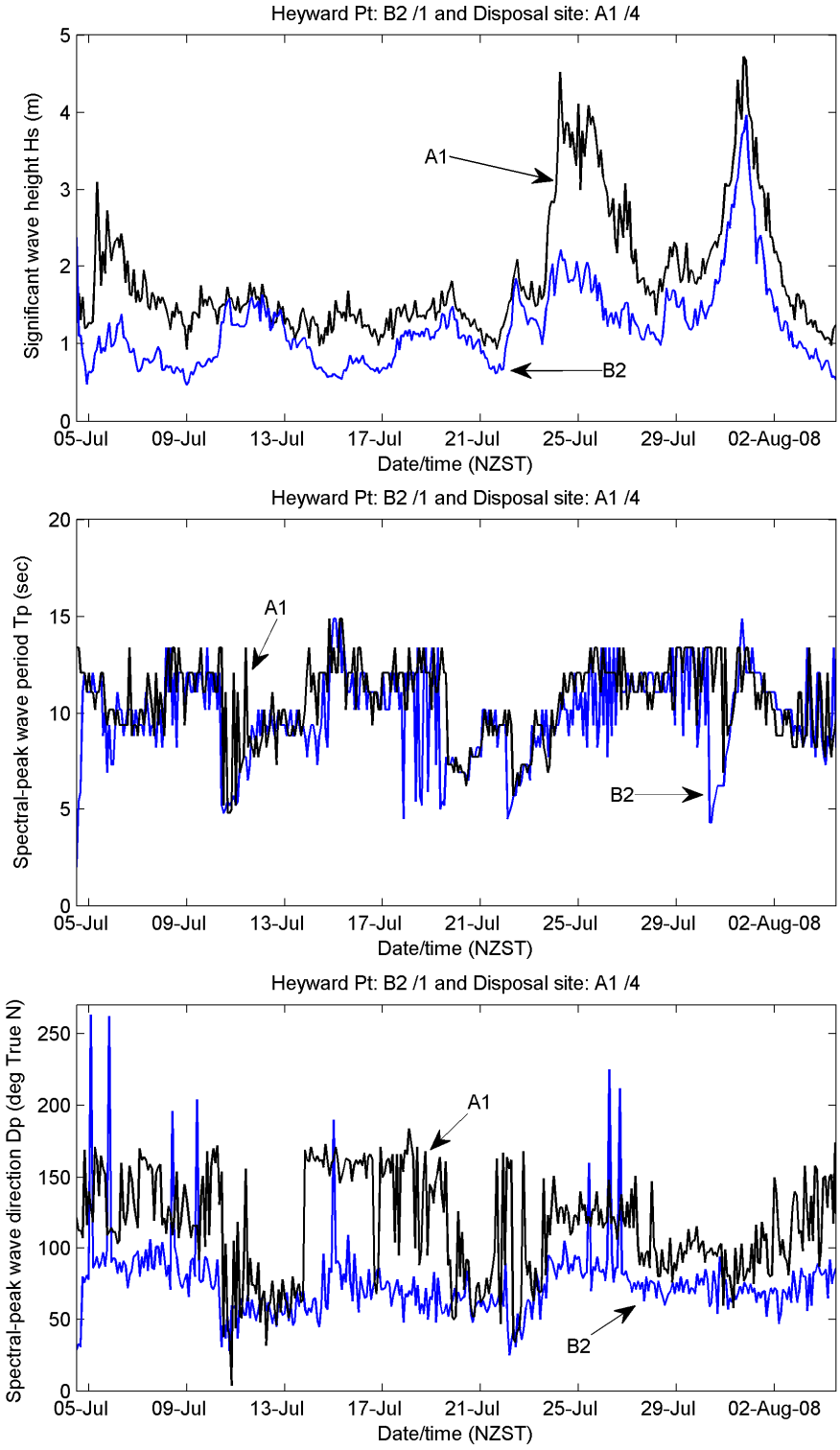

Figure 5.40: Wave statistics from both deployment B2 /1 (blue) and the offshore mooring A1 /4: (black) for: (top) significant wave height (H_s); (middle) spectral peak period (T_p); (bottom) spectral peak wave direction (D_p).

6. Summary

A full set of current and wave measurements has been obtained at a potential dredged-material disposal site at A1 (4 km northeast of Taiaroa Head) over a 4-month period from March to July 2008 (excluding gaps between deployments). For all but one of these deployments, a concurrent ADCP mooring site was also occupied at either B1 (Blueskin Bay) or B2 (Heyward Point). Inshore, waves were only measured at B2, due to a malfunction in the ADCP at site B1.

This report presents a detailed synthesis of the field measurements and draws out the key oceanographic and meteorological factors that explain the variability and extremes in the ADCP datasets.

The current velocity measurements provide a useful dataset in their own right, showing the prevailing patterns of coastal and shelf circulation in the area of Otago Heads. Tidal currents at all three ADCP sites were a small proportion of the measured currents. At A1, the prevailing current drift in most cases is to the SE, with a slight deviation to the south in the last deployment (July 2008). This prevailing current drift is altered at times when moderate to strong south to SE winds reverse the drift, but otherwise the more frequent winds from the SW and NE quadrants appear to sustain the south-easterly drift. Sometimes winds from a more northerly direction deviate this current drift slightly more towards the south at A1.

These results have implications for the hydrodynamic and sediment modelling for a disposal ground offshore (Bell et al. 2009), with tidal currents being negligible, the Southland Current providing the regional context for the net (mean) flows, including the possibility of an eddy off Otago Heads, and the winds being the predominant cause of variability of current drift in the area of A1.

In Blueskin Bay (B1), the net current drift was quite variable. For the first deployment in March/April 2008, the current drift exhibited slow cyclic meanders at the seabed arising from a succession of alternating NE and SW winds. This contrasts with the June 2008 deployment, where the current drift was more consistently towards the northerly quarter, due to more frequent and stronger winds from the SW and weaker less frequent winds from the NE.

Off Heyward Point (B2), the net current drift is generally eastwards at 1 km/day near the seabed. In a similar manner to site A1, south to SE winds can reverse the net drift at B2 to be in a more NW direction towards Blueskin Bay.

The current velocity measurements at various depths provide a reliable and consistent dataset for use in hydrodynamic, sediment-plume and sediment-transport models used to assess environmental effects in Bell et al. (2009).

Logged temperatures and some salinity-depth profiling indicated that weak density stratification can be present at times e.g., heating of surface waters in autumn and a small signature of reduced surface salinities (probably from the Clutha River). However, it was mainly confined to the top few metres of the water column, and is unlikely to affect the dispersal of dredged material released at the disposal site from a dredger with a draught of several metres. Temperature measurements were also used to bracket winter and late-summer estimates of settling velocity for sediment grains, with settling slightly slower in colder temperatures.

The three highest wave events for the field season all occurred during the last deployment. The highest significant wave height of 4.7 m was reached at 1800 h on 31 July 2008, with peak spectral periods of 11–13 seconds (swell) arriving from an easterly direction. Local winds at Taiaroa Head preceding this wave peak were from the SE. The second highest significant wave height of 4.5 m was reached a week earlier at 0600 h on 24 July 2008, with peak spectral periods of 10–12 seconds (swell) arriving from a SE direction, with local winds blowing from the south.

Wave statistics measured at A1 provide an essential dataset to verify wave models, which subsequently are required as input to sediment transport models. The wave information also provides a future resource for verifying any future wave forecasting system for the port operations.

Overall, these field datasets provide a coherent picture of the prevailing currents, waves and their variability in response to wind forcing on the inner shelf off Otago Heads. The extension of the field programme to a fourth deployment was worthwhile, capturing the three largest wave events for the entire field programme, and providing useful insights on the current drift at A1 when infrequent winds blow from the SE.

7. Acknowledgements

The authors wish to thank the following people for their field and data support: Allan Sutherland (POL) for his large input coordinating the local operations for mooring assembly and deployments with commercial divers and supplying wind/tide data; Kim Currie (NIWA/University of Otago) for CTD profiling; Andrew Willsman (NIWA, Dunedin) for assistance with ADCP deployments; Rod Budd (NIWA, Hamilton) for design and assembly of ADCP moorings; Scott Stephens and George Payne (NIWA, Hamilton) for downloading and analysis of wind and HOBO temperature data respectively; Aarno Korpela (NIWA, Wellington) for supplying archived satellite SST maps.

8. References

Bell, R.G.; Oldman, J.W.; Beamsley, B.; Green, M.O.; Pritchard, M.; Johnson, D.; McComb, P.; Hancock, N.; Grant, D.; Zyngfogel, R. (2009). Port of Otago dredging project: Harbour and offshore modelling. NIWA Client Report HAM2008-179 prepared for the Port Otago Ltd.

Bowman, H. (2008a). Deployment report, S4 current meter: 1 km north of Quarantine Point, Otago Harbour, May 2008. Dept. of Marine Science, University of Otago, 6 June 2008, 6 p.

Bowman, H. (2008b). Deployment report, S4 current meter: Raynbirds and Macandrew Bays, Otago Harbour, June–July 2008. Dept. of Marine Science, University of Otago, 12 November 2008, 11 p.

Sutton, P.J.H. (2003). The Southland Current: a sub Antarctic current. *New Zealand Journal of Marine and Freshwater Research 37*: 645–652.